



Unearthing the intersections: positivity bounds, weak gravity conjecture, and asymptotic safety landscapes from photon-graviton flows

Benjamin Knorr ^a and Alessia Platania ^b

^a*Nordita, Stockholm University and KTH Royal Institute of Technology, Hannes Alfvéns väg 12, SE-106 91 Stockholm, Sweden*

^b*Niels Bohr International Academy, The Niels Bohr Institute, Blegdamsvej 17, DK-2100 Copenhagen Ø, DENMARK*

E-mail: benjamin.knorr@su.se, alessia.platania@nbi.ku.dk

ABSTRACT: We compute the asymptotic safety landscape stemming from ultraviolet-complete photon-graviton flows in a field theoretic setup, and we confront it with the weak gravity conjecture and, for the first time, with positivity bounds. At fourth order in derivatives, we find two gravitational fixed points providing viable ultraviolet completions for the theory. One of them comes with a single relevant direction, which sets the scale of quantum gravity. The corresponding sub-landscape is a single point. The second fixed point yields a richer sub-landscape of effective theories, most of which is described by an approximately straight line in the space of dimensionless Wilson coefficients. We additionally discover that: *(i)* the two sub-landscapes are continuously connected via a small “candy cane” regime, and the whole asymptotic safety landscape falls onto a plane; this is consistent with earlier findings and could be a universal feature in Asymptotic Safety; *(ii)* in such a field-theoretic setup, the Euler coupling plays a special role, as it is unconstrained by quantum scale invariance, but can enter off-shell bounds such as entropy-based positivity constraints; *(iii)* Planck-scale-suppressed violations of both weak gravity and positivity bounds occur across the landscape. The latter result resonates with expectations grounded on effective field theory arguments.

Contents

1	Introduction	2
2	Landscapes, positivity bounds, and the weak gravity conjecture	5
2.1	Landscapes in String Theory and Asymptotic Safety	5
2.2	Positivity bounds	6
2.3	Entropy positivity bounds and electric weak gravity conjecture	8
3	Computing the AS landscape	9
3.1	Defining the Wilson coefficients	9
3.2	Fixed points, UV behavior, and free parameters	11
3.3	Fixed point structure	12
3.4	Computing the landscape: parameterizing the IR behavior of the flow	14
3.5	Sub-landscape from FP1	15
3.6	Sub-landscape from FP2	16
3.7	Sub-landscape from MFP	18
4	Comparing the AS landscape with positivity, entropy, and weak gravity bounds	19
5	Positivity bounds and WGC beyond Wilson coefficients: flowing conditions	23
6	Summary and conclusions	24
A	Photon-graviton flows: setup and definitions	28
A.1	The Functional Renormalization Group	28
A.2	Action, gauge fixing, regularization and field redefinitions	29
B	Analytic Wilson coefficient in the pure matter theory	30

1 Introduction

One of the most challenging open problems in theoretical physics is to understand the gravitational interaction at the smallest distance scales. At Planckian scales, we expect gravity to shed off its classical behavior and display quantum properties, similar to other gauge and matter fields. Different approaches to quantum gravity (QG) try to describe the phenomena at these scales starting from a variety of fundamental ideas and based on seemingly different frameworks. Fundamental research in each of these theories entails the investigation of their ultraviolet (UV) details and, ideally, the use of top-down strategies to derive predictions from scratch. Effective field theory (EFT), on the other hand, is a powerful mathematical formalism to describe physical phenomena involving particles and fields within a given energy range — usually below a given cutoff scale where new physics becomes relevant. It serves as a pragmatic approach for modeling complex systems while incorporating the effects of higher energy degrees of freedom or features through systematic expansions.

The challenge lies in bridging the gap between these two frameworks: QG, which governs the behavior of spacetime and gravitational interactions at the Planck scale, and EFT, which describes gravity-matter systems at much lower energy scales.

One way to connect QG to EFT is through decoupling [1]. This involves constructing EFTs that capture the low-energy dynamics of gravity while incorporating the effects of quantum fluctuations at shorter distances. By integrating out the high-energy modes, one can derive EFTs that manifest as low-energy approximations to the underlying QG theory. A paradigmatic example of this mechanism is realized within the Asymptotic Safety (AS) program for QG [2–11], which builds on the framework of quantum field theory (QFT), and on the idea that gravity could be UV-complete with respect to an interacting fixed point of the gravitational renormalization group (RG) flow. Within the AS approach, much effort has been put into corroborating the existence of this fixed point [12–14], as well as in assessing its unitarity [15–19], and its compatibility with matter [20–23]. Although RG trajectories have been found that connect the fixed point with the General Relativity (GR) regime, and despite the natural embedding of the decoupling mechanism in AS, a systematic study of the QG-EFT map in AS is missing. Similarly, most of the other QG approaches have devoted their main focus on understanding the UV details of the theory, often in isolation from matter.

The swampland program [24, 34] plays a crucial role in this endeavor, by providing constraints and guiding principles to construct EFTs that arise from consistent UV completions of gravity. At its core, the swampland program seeks to identify the theoretical constraints — formulated in terms of a set of conjectures — that any consistent quantum theory of gravity must satisfy. Its name, “swampland”, metaphorically reflects the idea that not all EFTs can arise from a consistent UV theory. The program aims to delineate which theoretical frameworks belong to the swampland of inconsistent theories, and which ones originate from fundamental theories. The latter set identifies the “landscape” of consistent EFTs. Whether such a landscape solely identifies consistent EFTs stemming from String Theory (ST), or more generally the set of EFTs generated by *any* consistent QG theory

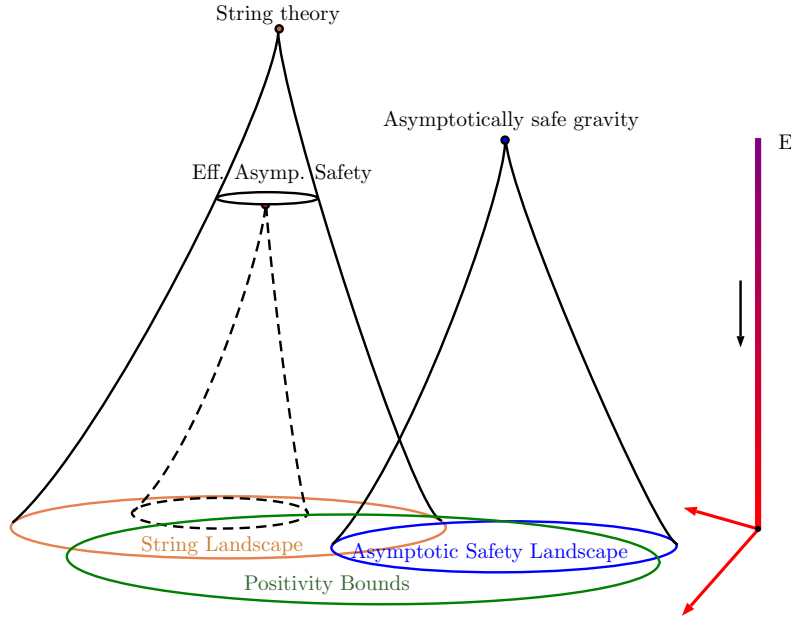


Figure 1. Sketch of the extensions of the swampland program [24] and the notion of landscape to other approaches to quantum gravity, in particular Asymptotically Safe Gravity. This paves the way to contrasting the asymptotic safety and string landscapes [25] and assessing the possibility of Asymptotic Safety being a low-energy approximation of String Theory [26–30], investigating the generality of swampland conjectures and string universality [31, 32], and testing Asymptotic Safety against important theoretical constraints such as positivity bounds [33].

is an open question. According to the String Lamppost Principle [31, 32], all such EFTs coming from consistent QG theories must have a stringy origin.

Although in the past years, the swampland program has sparked intense debate due to the use of conjectures, it has also inspired numerous research efforts. Its implications extend beyond the confines of ST, influencing broader discussions in cosmology, particle physics, and beyond [35–41]. In particular, despite the swampland program having emerged in the context of ST, the general idea of selecting and constraining the set of EFTs compatible with and stemming from different UV completions of gravity can [25], and should, be extended to other approaches to QG. Deriving the landscapes from different approaches could indeed allow for (i) a more efficient comparison with constraints derived from EFT [33], and (ii) a more direct and clean dictionary to compare the predictions of different QG approaches [42] and frameworks, which in the UV hardly talk to each other. Constructing the QG-EFT map and generalizing the notion of landscape to other QG theories [25] would additionally allow to investigate the validity of swampland conjectures beyond string models [25, 27, 43], and thus to test the String Lamppost Principle [31, 32]. In a similar direction, analyzing the intersections between different QG landscapes could reveal non-trivial connections between theories. For instance, if the AS landscape would lie inside the string landscape, or if the two would have a non-trivial intersection [25], this could indicate that AS be realized in the form of “effective AS” [26, 28], i.e., as a low-energy approximation of ST [27, 29, 30]. This

overarching idea that generalizes the big picture of the swampland program is illustrated in [Figure 1](#).

In this work, we take key steps in the realization of this program, by extending the investigations of [\[25\]](#) to a more sophisticated system and a full-fledged non-perturbative RG computation, and by comparing the AS landscape not only with swampland conjectures — specifically, the weak gravity conjecture (WGC) [\[44–47\]](#) — but also, for the first time, with positivity bounds [\[33\]](#). Concretely, we will focus on a photon-graviton system at fourth order in a derivative expansion, while only including couplings that cannot be removed by a local field redefinition. Explicitly, the dynamics is encoded in the effective action

$$\Gamma = \int d^4x \sqrt{g} \left[\frac{R}{16\pi G_N} + G_{\mathfrak{E}} \mathfrak{E} - \mathcal{F}_2 + G_{\mathcal{F}_2} (\mathcal{F}_2)^2 + G_{\mathcal{F}_4} \mathcal{F}_4 + G_{CFE} C^{\mu\nu\rho\sigma} F_{\mu\nu} F_{\rho\sigma} \right], \quad (1.1)$$

with

$$\mathcal{F}_2 = \frac{1}{4} F^{\mu\nu} F_{\mu\nu}, \quad \mathcal{F}_4 = \frac{1}{4} F^\mu{}_\nu F^\nu{}_\rho F^\rho{}_\sigma F^\sigma{}_\mu, \quad \mathfrak{E} = R_{\mu\nu\rho\sigma} R^{\mu\nu\rho\sigma} - 4R_{\mu\nu} R^{\mu\nu} + R^2. \quad (1.2)$$

Here, $F_{\mu\nu}$ is the Abelian field strength tensor and $C_{\mu\nu\rho\sigma}$ is the Weyl tensor. Along the lines of [\[25\]](#), we compute the beta functions and determine the AS landscape as the set of EFTs — parameterized by the relevant dimensionless Wilson coefficients — that are connected to UV-complete RG trajectories. We will then compare the Wilson coefficients in the landscape with standard positivity bounds [\[48, 49\]](#) and with a family of entropy-based positivity constraints [\[50\]](#), which contains the WGC for black holes in the presence of higher derivatives [\[50–52\]](#) as a particular case.

Our system has two viable gravitational UV fixed points, hence the AS landscape consists of two sub-landscapes. One fixed point comes with a single relevant direction, so that, once the scale of QG is fixed, the resulting sub-landscape is a zero-parameter theory: a single point in the space of dimensionless Wilson coefficients. The second fixed point has two relevant directions, so that the corresponding sub-landscape is a line. In particular, this line is nearly straight. The straight approximation only ceases to work in a small region where the sub-landscape of the second fixed point bends to continuously connect to the single-point sub-landscape coming from the most predictive fixed point. Globally, the entire AS landscape falls onto a plane — a feature already observed in a previous work [\[25\]](#). Whether this is a coincidence or a universal feature of AS is to be assessed by more extensive studies.

In agreement with general expectations from EFT [\[53–56\]](#), we find that Planck-scale suppressed violations of weak gravity and positivity constraints can occur across the landscape. We will show that such violations are minimized by the most predictive sub-landscape. Finally, our work also highlights the special role played by the Euler coupling in AS: while it is attached to a topological invariant and is thus generally unconstrained by the RG flow [\[57, 58\]](#), it can enter off-shell positivity constraints such as those based on black hole entropy [\[50\]](#). Such positivity bounds can thus entail constraints on the Euler coupling, rather than tests of AS.

Our paper is organized as follows. In [Section 2](#), we discuss the concepts that are important to this work in more detail: landscapes, positivity bounds, and the weak gravity

conjecture. [Section 3](#) contains our results on the fixed point structure, and an in-depth discussion of the ensuing landscapes. With these results in hand, in [Section 4](#) and [Section 5](#) we confront our results with positivity, entropy, and weak gravity bounds. Finally, in [Section 6](#) we summarize and discuss our results. The two appendices contain some more details about our technical setup and an analytical result.

2 Landscapes, positivity bounds, and the weak gravity conjecture

This section introduces the basic concepts that we will need and use throughout the manuscript. This includes the notion of landscapes in QG and an overview of the weak gravity and positivity bounds that we will intersect with the AS landscape.

2.1 Landscapes in String Theory and Asymptotic Safety

The concept of landscape was first introduced in the context of ST [\[24\]](#), to indicate the set of infrared (IR) EFTs that admit a consistent UV completion in the presence of gravity. The swampland is the complement of this set — that is, the set of EFTs that cannot be UV-completed when coupled to gravity. The difficulties in tracing the set of theories belonging to the string landscape via top-down derivations have led to the idea at the core of the swampland program [\[34\]](#): to determine the conditions or criteria that precisely select the EFTs belonging to the landscape. Such conditions are better known as “swampland conjectures”, and stem from recurring patterns in stringy constructions, black hole physics, and the interrelations between different conjectures. In the following, we will assume that swampland conjectures precisely identify the string landscape.

While the concept of landscape — seen as the set of EFTs stemming from consistent gravity-matter UV completions — is universal, the strategy to determine it may depend on the specific approach to QG. For a given approach to QG, the goal is to predict the set of allowed Wilson coefficients in the corresponding low-energy EFT. The first generalization of the concept of the QG landscape beyond ST has been put forth in [\[25\]](#), in the context of AS [\[59\]](#). As argued in [\[25\]](#), the AS version of the string landscape is the set of Wilson coefficients in the effective action stemming from asymptotically safe RG trajectories, cf. [Figure 2](#). If more than one UV fixed point exists, we will define the landscape as the union of the “sub-landscapes” identified by each viable UV fixed point. These sub-landscapes are in general not contiguous, but can never overlap: they will typically be disjoint sets.

It is noteworthy that the concept of landscape in AS is amenable to explicit computation. The Functional Renormalization Group (FRG) [\[60\]](#) (see [Appendix A](#) for a brief review) is typically used in the field of AS to corroborate the existence of interacting fixed points of the RG flow, i.e., possible UV completions of the theory. In a nutshell, the idea of the FRG is to perform the path integral in the Wilsonian spirit by integrating out modes above an IR cutoff scale k . All couplings thus acquire an RG-scale dependence, and in the limit $k \rightarrow 0$ — corresponding to all fluctuations having been integrated out — the standard effective action Γ is obtained. As a consequence, the FRG also provides a clear recipe to compute the Wilson coefficients belonging to the landscape [\[25\]](#): they are the IR ($k \rightarrow 0$) limits of the FRG-running couplings $G_i(k)$, for all RG trajectories departing from a given

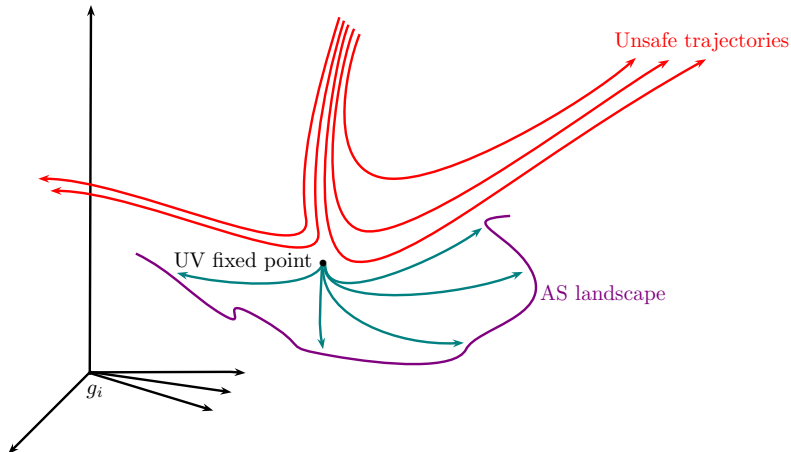


Figure 2. Generalization of the concept of landscape to AS. In the space of dimensionless running couplings, the flow is controlled by one or more fixed points (black dot). Each fixed point with at least one UV-attractive direction corresponds to a possible UV completion. RG trajectories whose UV behavior is not governed by a fixed point (red lines) correspond to non-renormalizable theories. Asymptotically safe trajectories (petrol-green lines) are those starting at a fixed point in the UV. The AS landscape stemming from a given fixed point (purple line) is the set of IR endpoints of these trajectories.

fixed point. We shall return to this point in the next section, in the light of the definitions of positivity and entropy-based bounds.

2.2 Positivity bounds

Positivity bounds originally arose in the context of EFT. The underlying idea is that consistency conditions for a fundamental theory, including locality, unitarity, analyticity, and Lorentz invariance, constrain the scattering amplitudes of the theory, even at scales above the cutoff where the EFT is valid. More precisely, *without* knowing the details of the UV completion of the EFT, one can still infer constraints on the IR physics that follow from these consistency conditions. One strategy for deriving positivity bounds is to use the optical theorem together with the (assumed or known) branch cut and pole structure of scattering amplitudes in order to find contour integrals that are positive. This can then be mapped onto constraints on specific combinations of Wilson coefficients that are, by construction, gauge- and reparameterization-invariant. For a recent overview of the topic, see e.g. [33]. For the theory that we consider in this work, the effective action is given by (1.1), and the relevant dimensionless Wilson coefficients are

$$w_{\mathcal{F}_2} = \frac{G_{\mathcal{F}_2}}{(16\pi G_N)^2}, \quad w_{\mathcal{F}_4} = \frac{G_{\mathcal{F}_4}}{(16\pi G_N)^2}, \quad w_C = \frac{G_{CFF}}{16\pi G_N}, \quad (2.1)$$

Positivity bounds on these coefficients have been discussed e.g. in [48, 49]. In [49], bounds for the first two Wilson coefficients were derived, together with constraints for other operators that we do not consider in this work. With the EFT cutoff Λ , the dimensionless

quantities

$$f_2 = \frac{(16\pi G_N)^2 \Lambda^4}{2} (w_{\mathcal{F}_2^2} + w_{\mathcal{F}_4}), \quad g_2 = \frac{(16\pi G_N)^2 \Lambda^4}{2} (w_{\mathcal{F}_2^2} + 3w_{\mathcal{F}_4}), \quad (2.2)$$

need to satisfy

$$g_2 > |f_2|. \quad (2.3)$$

On the other hand, in [48], also the third Wilson coefficient has been included, and the scale has been chosen explicitly in terms of the Planck scale. The two bounds of [48] read¹

$$w_{\mathcal{F}_2^2} + 2w_{\mathcal{F}_4} - 2|w_C| > 0, \quad (2.4)$$

$$w_{\mathcal{F}_4} > 0. \quad (2.5)$$

It is however important to stress that most of the literature, including the above works, explicitly excludes the massless graviton in the derivation of positivity bounds. This is partially related to the technical difficulties originating from subtracting the massless graviton pole and treating the IR logarithms. In connection to our work, this has two important implications. First, while there has been some effort in addressing these issues, see e.g. [48, 53, 54, 61, 62], the situation is not settled yet. In particular, since we allow for massless graviton fluctuations, we will observe a logarithmic running in the IR, and we will have to discuss how to treat the resulting logarithms in our RG flow when defining the Wilson coefficients. Second, and most importantly, it is not obvious that the strict inequalities above also apply to theories with massless degrees of freedom. The expectation [53–55] is that such positivity bounds may be violated once gravity is turned on. The violation would result in a weakening (or even a complete removal [56]) of the positivity bounds: sums of dimensionless Wilson coefficients which ought to be positive in unitary, gravity-free theories, could actually be slightly negative [53–55]. The amount of allowed violations is not precisely settled but, when present [56], it is generally expected to be an $\mathcal{O}(1)$ quantity in appropriate units.

Specifically, within our system given by the action (1.1), any potential violation of positivity bounds should naturally be Planck-mass suppressed, as long as the dimensionless Wilson coefficients (2.1) are of $\mathcal{O}(1)$. To illustrate this argument, let us consider photon-photon scattering. With our effective action (1.1), the two-to-two scattering amplitude in the low energy and forward scattering limit reads, structurally [63],

$$\mathcal{A} \sim -G_N \frac{s^2}{t} + c s^2 + \dots, \quad (2.6)$$

where the first term originates from the massless graviton pole, c is a linear combination of the couplings $G_{\mathcal{F}_2^2}$ and $G_{\mathcal{F}_4}$, and s, t are the standard Mandelstam variables. Positivity bounds are tied to the positivity of c . Using our definitions for the dimensionless Wilson coefficients (2.1), and assuming $w_i \sim -\mathcal{O}(1)$, we have that

$$\mathcal{A} \sim -G_N \frac{s^2}{t} - \mathcal{O}(1) G_N^2 s^2 + \dots \sim -\frac{s^2}{t M_{Pl}^2} - \mathcal{O}(1) \frac{s^2}{M_{Pl}^4} + \dots \quad (2.7)$$

¹The first of these two bounds actually originates from two independent constraints, namely $w_{\mathcal{F}_2^2} + 2w_{\mathcal{F}_4} - 2w_C > 0$ and $w_{\mathcal{F}_2^2} + 2w_{\mathcal{F}_4} + 2w_C > 0$, whose combination gives the first bound.

This entails that, as long as energies do not reach the Planck scale, $s \ll M_{Pl}^2$, any potential violation is suppressed significantly. As a matter of fact, if a second mass scale $M \ll M_{Pl}$ is present, it is conjectured that only a weaker positivity bound needs to be fulfilled [63],

$$c \gtrsim -\frac{\mathcal{O}(1)}{M^2 M_{Pl}^2}, \quad (2.8)$$

compared to which any potential violation in our system is once again suppressed by a factor of M^2/M_{Pl}^2 .

2.3 Entropy positivity bounds and electric weak gravity conjecture

The WGC is among the most important and best-understood criteria within the swampland program. In the context of ST, it is strictly related to the No Global Symmetries conjecture, but it can also be motivated by the requirement that no black hole remnants are formed, since they might lead to consistency issues at the EFT level [44]. In its simplest form, its electric version states that in any consistent $U(1)$ -theory coupled to gravity, there must be at least one electrically charged state, whose dimensionless mass-to-charge ratio is bounded by an order-one number,

$$m \leq \sqrt{2} Q M_{Pl}, \quad (2.9)$$

where $Q = qg$ is the unquantized charge of the state with mass m , and g is the $U(1)$ -gauge coupling. Equivalently, there must be an electrically charged state whose charge-to-mass ratio is bounded by that of an extremal charged black hole,

$$Q/M \leq Q_{extr}/M_{extr}. \quad (2.10)$$

At variance with the condition (2.9), the bound above is not universal, rather it is generally modified by higher derivative terms in the effective action, in the gravitational or in the $U(1)$ sector [50–52]. Specifically, in a generic photon-graviton EFT, the condition (2.9) becomes

$$Q/M \leq Q_{extr}/M_{extr} \left(1 - \frac{\Delta}{M^2} \right), \quad (2.11)$$

where Δ entails a non-trivial combination of Wilson coefficients, and the extremality parameter is in the range $\xi = \sqrt{1 - Q^2/M^2} \in [0, 1]$, or in $[0, 1/2]$ for black holes with positive specific heat [50]. Following the derivations in [50–52], for a theory of the type (1.1) considered in this paper, the combination reads [50]

$$\Delta = (1 - \xi)^2 d_0 + 20\xi(8\pi G_N)G_{\mathfrak{e}} - 5\xi(1 - \xi)(16\pi G_N G_{\mathfrak{e}} + G_{CFF}), \quad (2.12)$$

with

$$d_0 = \frac{G_{\mathcal{F}_2^2}}{32\pi G_N} + \frac{G_{\mathcal{F}_4}}{16\pi G_N} - G_{CFF} = 8\pi G_N (w_{\mathcal{F}_2^2} + 2w_{\mathcal{F}_4} - 2w_C), \quad (2.13)$$

and must be non-negative for all ξ in the allowed range for the entropy-positivity-bounds in [50] to be fulfilled. We note that despite the Euler coupling $G_{\mathfrak{e}}$ not entering field equations or scattering amplitudes — at least not trivially — it can affect off-shell quantities like the

black hole entropy. Thus, it can generally impact the family of positivity bounds attached to the condition

$$\Delta > 0. \quad (2.14)$$

Nonetheless, $G_{\mathfrak{E}}$ non-trivially drops out of the linear combination of Wilson coefficients d_0 , which is strictly related to the electric WGC. Indeed, in the case of a highly charged black hole ($\xi \ll 1$), the family of positivity bounds (2.14) is proportional to the extremality condition of charged black holes [50] and yields the electric WGC for black holes in the presence of higher-derivative corrections [51]

$$d_0 > 0. \quad (2.15)$$

This is the condition that we will consider in this manuscript. Similarly to positivity bounds, in the presence of gravitational quantum fluctuations, small violations of the WGC are allowed and compatible with unitarity and causality [55].

3 Computing the AS landscape

In this section, we compute the landscape of EFT stemming from asymptotically safe photon-gravity flows. The dynamics is encoded in the action (1.1). For the computation of the beta functions, we will work with its Euclidean counterpart,

$$\Gamma_k = \int d^4x \sqrt{g} \left[-\frac{R}{16\pi G_N} + G_{\mathfrak{E}} \mathfrak{E} + \mathcal{F}_2 + G_{\mathcal{F}_2^2} (\mathcal{F}_2)^2 + G_{\mathcal{F}_4} \mathcal{F}_4 + G_{CFF} C^{\mu\nu\rho\sigma} F_{\mu\nu} F_{\rho\sigma} \right], \quad (3.1)$$

where all couplings $G_i(k) \equiv \{G_N, G_{\mathfrak{E}}, G_{\mathcal{F}_2^2}, G_{\mathcal{F}_4}, G_{CFF}\}$ now depend on the RG scale k . As remarked in the introduction, we work in the same spirit as in the EFT literature and remove all inessential operators across all scales by an appropriate k -dependent field redefinition [64, 65] (see Appendix A for additional details).

3.1 Defining the Wilson coefficients

As anticipated in Section 2.1, identifying the AS landscape boils down to computing the set of IR endpoints ($k \rightarrow 0$ limit of the FRG flow) of all asymptotically safe trajectories [25] (cf. Figure 2). Each endpoint corresponds to an EFT in the landscape, and is uniquely described by the (generally dimensional) Wilson coefficients

$$W_{G_i} \equiv \lim_{k \rightarrow 0} G_i(k). \quad (3.2)$$

The flow has to be computed for the dimensionless counterparts of the couplings $G_i(k)$, i.e.,

$$g(k) = G_N(k) k^2, \quad g_{\mathcal{F}_2^2}(k) = G_{\mathcal{F}_2^2}(k) k^4, \quad g_{\mathcal{F}_4}(k) = G_{\mathcal{F}_4}(k) k^4, \quad g_{CFF}(k) = G_{CFF}(k) k^2. \quad (3.3)$$

The flow for these four dimensionless couplings has been computed with the help of the Mathematica package xAct [66–68] and a well-tested code [69–71]. Some details on the computation are reported in Appendix A. The complete set of beta functions can be found in the accompanying notebook [72].

In terms of the above running dimensionless couplings, the dimensionless Wilson coefficients in (2.1) originate from the following limits

$$\begin{aligned}
w_{\mathcal{F}_2^2} &= \lim_{k \rightarrow 0} \frac{g_{\mathcal{F}_2^2}(k)}{(16\pi g(k))^2} \equiv \lim_{k \rightarrow 0} \frac{G_{\mathcal{F}_2^2}(k)}{(16\pi G_N(k))^2}, \\
w_{\mathcal{F}_4^2} &= \lim_{k \rightarrow 0} \frac{g_{\mathcal{F}_4^2}(k)}{(16\pi g(k))^2} \equiv \lim_{k \rightarrow 0} \frac{G_{\mathcal{F}_4}(k)}{(16\pi G_N(k))^2}, \\
w_C &= \lim_{k \rightarrow 0} \frac{g_{CFF}(k)}{16\pi g(k)} \equiv \lim_{k \rightarrow 0} \frac{G_{CFF}(k)}{(16\pi G_N(k))}.
\end{aligned} \tag{3.4}$$

These are the dimensionless ratios of couplings that enter scattering amplitudes in our system, and thus the corresponding positivity bounds. However, some caveats and ambiguities remain. Hence, prior to computing the AS landscape, we need to discuss some aspects of the definition of the Wilson coefficients in our setup:

- **Wick rotation:** Our computation of beta functions has been performed with Euclidean signature, as is the standard in the field (for recent progress in defining flows directly in Lorentzian signature, see [17]). We thus have to perform a Wick rotation to relate our couplings to the couplings in the literature on positivity bounds and the WGC [48–50]. It is known that the Wick rotation comes with many issues in gravitational theories [73]. We implement the Wick rotation pragmatically by the rule that spacetime curvature tensors get a minus sign, and field strength tensors a factor of i . In practice, this only affects the Einstein-Hilbert term and the kinetic term of the photon in our action. As the end result of this procedure, our couplings do not have to be modified and can be used directly in all bounds.
- **Definition of Wilson coefficients in the presence of logarithms:** Some of the couplings in our system display a logarithmic running originating from massless graviton fluctuations. Such a logarithmic running introduces an ambiguity in the definition of the Wilson coefficients, since one can always redefine the scale in the logarithm, so that $a_1 + \log(k^2/k_1^2) = a_2 + \log(k^2/k_2^2)$. This makes it necessary to adopt a prescription to subtract the logarithm and thus to define the Wilson coefficients uniquely (see also [25]).

Grounded on this issue, and in anticipation of the results, it turns out useful to introduce the two combinations

$$g_{\pm}(k) = \frac{g_{\mathcal{F}_2^2}(k) \pm g_{\mathcal{F}_4}(k)}{2}, \tag{3.5}$$

and the corresponding dimensionless Wilson coefficients

$$w_{\pm} = \lim_{k \rightarrow 0} \frac{g_{\pm}(k)}{(16\pi g(k))^2} \equiv \lim_{k \rightarrow 0} \frac{G_{\pm}(k)}{(16\pi G_N(k))^2}. \tag{3.6}$$

The underlying reason is that both $g_{\mathcal{F}_2^2}$ and $g_{\mathcal{F}_4}$ run logarithmically in the IR, but with opposite signs. Thus, in combining them, only g_- shows a logarithmic running

in the IR, whereas g_+ does not, allowing us to eliminate one of the two logarithmic ambiguities.

In practice, we will subtract the logarithmic running to obtain the Wilson coefficient w_- . To parameterize the ambiguity, we will fix our reference scale to be the Planck mass and introduce a parameter, c_l , multiplying G_N inside the logarithm:

$$w_- \equiv \frac{1}{2}(w_{\mathcal{F}_2^2} - w_{\mathcal{F}_4^2}) - N \ln [c_l G_N k^2] . \quad (3.7)$$

In computing the landscape, N has to be chosen appropriately to remove the universal IR logarithmic running. This will be shown explicitly in [Section 3.4](#), cf. (3.11c). Different choices of c_l then correspond to different prescriptions to subtract the logarithm and define the Wilson coefficient w_- .

- Role of Euler coupling** In four dimensions, the Euler term \mathfrak{E} is topological, and thus the corresponding coupling $G_{\mathfrak{E}}$ does not enter the right-hand side of the flow equation in conventional treatments. There are two consequences to this. First, the coupling will generically not show a fixed point [57], but run off to $\pm\infty$ for $k \rightarrow \infty$. Modulo the reconstruction problem [74–76], this suggests that certain topologies are preferred in the Euclidean path integral, or that only topologies with vanishing Euler term contribute to the Lorentzian path integral [58]. Second, even disregarding the first issue, without any additional constraint we cannot uniquely define the Wilson coefficient of the Euler coupling, as it can be shifted by an arbitrary amount while still fulfilling the same RG equation. This problem is exacerbated by the fact that the coupling also runs logarithmically in the IR, giving rise to the same ambiguity as for g_- . This is generally not a problem, as the Euler coupling typically does not enter scattering amplitudes in four dimensions. Nonetheless, as we shall see, the above issues lead to ambiguities at the level of the bounds involving off-shell quantities.

With these caveats and ambiguities in mind, in the next subsections, we will continue our discussion by investigating the analytical properties of two important limits of the FRG flow: the fixed point structure in the UV, and its universal running in the IR.

3.2 Fixed points, UV behavior, and free parameters

Obtaining the AS landscape requires in the first place a UV fixed point from which the flow emanates. The fixed points of the RG flow are given by the zeros of the vector field of beta functions $\vec{\beta}(\vec{g})$ of all dimensionless couplings \vec{g} . Along with the fixed points, the leading-order behavior of the flow about a fixed point contains information about the predictivity of the corresponding theory, which, in turn, is related to the dimensionality of the corresponding sub-landscape. Indeed, linearizing the beta functions about a fixed point \vec{g}^* and solving the flow yields the leading-order scaling

$$\vec{g} = \vec{g}^* + \sum_i c_i \vec{e}_i \left(\frac{k}{k_0} \right)^{-\theta_i} , \quad (3.8)$$

where the \vec{e}_i are the unit eigenvectors of the stability matrix $\partial\vec{\beta}/\partial\vec{g}$, the c_i are integration constants, k_0 is an arbitrary reference scale, and the critical exponents θ_i are defined as minus the eigenvalues of the stability matrix defined above. The number of relevant directions equates to the number of positive critical exponents and measures the predictivity of the theory generated by the UV fixed point: RG trajectories reaching the fixed point in the limit $k \rightarrow \infty$ are those whose integration constants c_i multiplying a positive power of k are zero. Thus, the fewer the number of relevant directions for a fixed point, the fewer the number of integration constants to vary to identify an RG trajectory, resulting in a higher predictive power.

For asymptotically safe trajectories, the number of non-vanishing integration constants equates to the number N of relevant directions of the flow. We note however that one of the integration constants associated with the relevant couplings can be absorbed to redefine the reference scale,

$$k_T \equiv c_i^{1/\theta_i} k_0. \quad (3.9)$$

The possibility of redefining the reference scale, or, equivalently, adding an arbitrary shift to the RG time $t = \log(k/k_0)$ is related to the invariance of the flow under shifts of the RG time t . At the same time, k_T has the interpretation of a transition scale from the fixed point (or, QG) regime to the IR scaling. Indeed, as we shall see in this section, in a gravitational theory k_T is also the mass scale defining the Newton coupling.

In any theory with dimensionful couplings, one needs at least one arbitrary unit mass scale with respect to which other dimensionful quantities can be measured: one of the integration constants of the full theory can be eliminated to define such a scale. Thus, contrary to the common folklore that N relevant directions correspond to N free parameters to be measured to fix the theory, the need to have a unit of measure reduces the number of free parameters to $N - 1$ *dimensionless* quantities. This number also defines the dimensionality of the landscape in the space of dimensionless Wilson coefficients. The only exception to this argument are scale-free theories. If our universe were a conformal field theory, then all measurable quantities would be dimensionless, in which case the need to introduce one arbitrary mass unit scale would disappear.

Following this general discussion, in the next subsection we shall present the fixed point structure for our system.

3.3 Fixed point structure

The beta functions for the dimensionless couplings $\{g, g_+, g_-, g_{CFE}\}$ are rational functions, and their fixed points correspond to their common zeros. Here we are excluding the Euler coupling $g_{\mathfrak{E}}$ from the set, since by construction its beta function can only vanish if all other couplings conspire so that $\beta_{g_{\mathfrak{E}}} = 0$. This is because, as mentioned in [Section 3.1](#), the Gauss-Bonnet operator \mathfrak{E} is a topological invariant and thus the Euler coupling cannot enter the right-hand side of the flow equation. As a consequence, $g_{\mathfrak{E}}$ cannot influence the flow of the other couplings, nor of itself, and hence it generically has no fixed points [[57](#), [58](#)].

The fixed points of our system that are reliable in our approximation are reported in [Table 1](#), together with the corresponding critical exponents. Despite the beta functions

	g^*	g_+^*	g_-^*	g_{CFE}^*	θ_i
GFP	0	0	0	0	$\{-4, -4, -2, -2\}$
MFP	0	-12.577	-10.383	-0.0901	$\{4.227, -0.477, -0.723, -1.041\}$
FP1	0.131	0.351	3.327	0.00375	$\{1.845, -0.239 \pm 0.0155i, -0.291\}$
FP2	0.126	-0.308	4.001	-0.00410	$\{1.936, 0.184, -0.141, -0.236\}$

Table 1. Overview of relevant fixed points (those that are both UV-complete and connected to the GFP in the IR), with their coordinates g_i^* in theory space and their critical exponents θ_i .

being rational functions, the search for fixed points generally requires resorting to numerical methods. Yet, when turning off Newton’s coupling, $g = 0$, one can find the zeros of the remaining three beta functions analytically. This identifies the “pure” matter fixed points (MFPs). Next to the standard GFP (first entry in Table 1), with critical exponents θ given by the classical mass dimensions of the couplings, we find two real MFPs. The first one is denoted by “MFP” in Table 1, and has a single relevant direction. The second one has highly non-canonical critical exponents, making it unreliable in our approximation, and it is also shielded from the GFP by a singularity in the beta functions, meaning that it cannot have a standard IR behavior. We thus excluded this second matter fixed point from Table 1.

To search for fully interacting fixed points, we employed a numerical fixed point search together with a random grid of starting points for the Newton-Raphson iteration, focusing on the region close to the GFP. For this, we first used a hypercube around the GFP with 10^6 randomly distributed starting points. We then successively enlarged the cuboid in all directions, except the g -direction, which we restricted to the interval $[0, 2\pi]$. This is because, on the one hand, we are only interested in fixed points with positive Newton’s coupling, and on the other hand, there is a singular line at $g = 2\pi$ in the flow, beyond which fixed points cannot be connected to a standard IR behavior.² The largest cuboid that we investigated was $g \in [0, 2\pi]$, $g_{\pm} \in [-100\pi^2, 100\pi^2]$, $g_{CFE} \in [-100, 100]$.³

With this method, we identified two reliable fixed points that are connected to the GFP in the IR. Both are displayed in Table 1. The first one (FP1) comes with a single relevant direction, and thus gives rise to the most predictive theory. By contrast, the second fixed point (FP2) has two relevant directions, with a peculiar magnitude of the two relevant critical exponents: θ_1 is an order of magnitude larger than θ_2 . We anticipate here that this makes the computation of the sub-landscape resulting from this fixed point numerically challenging.

Finally, in agreement with the discussion above and previous computations in AS [19, 58, 70, 71], we find that

$$k\partial_k g_{\mathfrak{E}}(k) > 0, \quad (3.10)$$

²This should be understood as a maximum value for the first singularity encountered when increasing g from 0 to positive values, and it stems from our renormalization condition for λ , see Appendix A.

³The factors of π are chosen for convenience — rescaling the couplings $\{g, g_{\pm}, g_{CFE}\} \rightarrow \{\pi\tilde{g}, \pi^2\tilde{g}_{\pm}, g_{CFE}\}$ removes all factors of π in the beta functions.

at both FP1 and FP2. This entails that the coupling $g_{\mathfrak{E}}$ runs to $+\infty$ for $k \rightarrow \infty$, and does not have a common fixed point with the other couplings, as expected.

To summarize, our system has three fixed points that can serve as a UV completion of the theory, and that are connected to the GFP ($g_i = 0$) in the IR.⁴ For the case of fully interacting fixed points (FP1 and FP2), this is needed to recover GR at low energies. The MFP, lying at $g^* = 0$, instead corresponds to a gravity-free UV completion of self-interacting photons. In the next subsections, we will show how to parameterize the IR behavior of the flow, which is key to compute the sub-landscapes stemming from the three possible UV completions presented in this subsection. In particular, an important role will be played by the so-called “separatrices” — critical RG trajectories connecting couples of fixed points and separating different behaviors of the flow. In the next subsections, we will describe the sub-landscapes identified by the three interacting fixed points in [Table 1](#), as well as the global geometry of the AS landscape.

3.4 Computing the landscape: parameterizing the IR behavior of the flow

Parameterizing the IR behavior of the beta functions is a necessary step to efficiently compute the AS landscape. The strategy is to expand the beta functions in the IR about the GFP by using ansätze $a(k/k_0)^{-d_c}(b + c \log(k/k_{ref}))$ for the running of the couplings, with d_c being the classical mass dimension of the corresponding coupling. Inserting these into the beta functions, one then extracts the coefficients a, b, c . This procedure yields the following scalings in the limit $k \rightarrow 0$, which are IR-universal, i.e., independent of the specific UV completion:

$$g(k) \simeq g_{IR} \left(\frac{k}{k_0} \right)^2, \quad (3.11a)$$

$$g_+(k) \simeq g_{IR}^2 \left(\frac{k}{k_0} \right)^4 f_+, \quad (3.11b)$$

$$g_-(k) \simeq g_{IR}^2 \left(\frac{k}{k_0} \right)^4 \left(f_- - \frac{548}{15} \ln \left[c_l g_{IR} \left(\frac{k}{k_0} \right)^2 \right] \right), \quad (3.11c)$$

$$g_{CFF}(k) \simeq g_{IR} \left(\frac{k}{k_0} \right)^2 f_c. \quad (3.11d)$$

In this, c_l parameterizes the ambiguity in defining the argument of the logarithm, in accordance with the discussion in [Section 3.1](#). The remaining parameters $\{f_{\pm}, f_c\}$ are to be determined by the RG flow: they depend on the fixed point one starts with and on the specific RG trajectory departing from it. As the running dimensionful Newton coupling is $G(k) \equiv g(k)k^{-2}$, the combination $g_{IR}k_0^{-2}$ defines the Newton coupling as

$$G_N \equiv \lim_{k \rightarrow 0} g(k)k^{-2} = g_{IR}k_0^{-2}. \quad (3.12)$$

⁴For general theories including couplings with positive mass dimension (e.g., a cosmological constant), the condition of a UV fixed point being connected to the GFP generalizes to the existence of RG trajectories departing from it and reaching or passing close to the GFP in the IR.

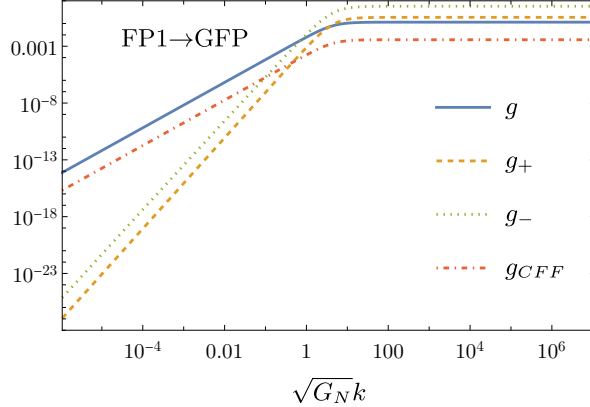


Figure 3. Flow of all dimensionless couplings along the only RG trajectory emanating from FP1 and reproducing GR at low energies, i.e., the separatrix joining FP1 and GFP. The running is shown as a function of the FRG scale k in Planck units, with a logarithmic scale on both axes. One can clearly see the scaling regimes of the two fixed points: for $k \gtrsim G_N^{-1/2}$, the couplings flow towards their fixed point values, whereas for $k \lesssim G_N^{-1/2}$, they run according to their mass dimensions.

In turn, G_N sets the scale of QG, and thereby provides a scale with respect to which all other dimensionful quantities can be meaningfully defined. Indeed, while the unit scale G_N is arbitrary, all other Wilson coefficients can be defined by the dimensionless ratios (3.4) and (3.6) — the only quantities that are relevant to assess positivity bounds.

3.5 Sub-landscape from FP1

The most predictive UV completion in our setup is provided by FP1, as it comes with one relevant direction only. The free parameter attached with its only relevant direction fixes the scale of QG, G_N , and thereby also fixes the units to define all other Wilson coefficients. All remaining dimensionless Wilson coefficients are thus predicted uniquely.

The single relevant direction and the presence of an IR fixed point (the GFP) imply that there are only two trajectories emanating from FP1: one diverging, and one approaching the GFP, as $k \rightarrow 0$. The latter trajectory (or, more precisely, the family of trajectories for different values of the QG scale) corresponds to the separatrix between FP1 and the GFP in theory space. The flow of the dimensionless couplings along this separatrix is shown in Figure 3.

The sub-landscape stemming from FP1 is thus a single point, and it corresponds to the $k \rightarrow 0$ limit of the FP1-GFP separatrix. The separatrix can be computed numerically by integrating the beta functions with initial conditions close to FP1, perturbed in the direction of the eigenvector corresponding to the positive critical exponent. The only EFT in the sub-landscape is identified by the following Wilson coefficients:

$$w_+ = 0.00792, \quad w_C = 0.000550. \quad (3.13)$$

The Wilson coefficient of w_- suffers the aforementioned ambiguity due to its logarithmic running. Trivially, this coefficient depends logarithmically on the parameter c_l . For $c_l =$

16π , we obtain

$$w_- = 0.0955. \quad (3.14)$$

We shall use these Wilson coefficients in the next section to investigate the compatibility with positivity bounds and the weak gravity conjecture.

3.6 Sub-landscape from FP2

We move on to discuss the sub-landscape connected to FP2. This fixed point has two relevant directions. Following from the earlier discussion that one of the free parameters sets the QG scale, the ensuing sub-landscape is one-dimensional: it is a line in the space of dimensionless Wilson coefficients. Here, all RG trajectories fall into three classes: those that approach the GFP in the IR, those that diverge, and the two boundary trajectories between these two behaviors. The first set makes up the sub-landscape.

Before we discuss our results, let us briefly point out a technical difficulty. Since the positive critical exponents of this fixed point are one order of magnitude apart, see [Table 1](#), the numerical determination of the sub-landscape requires high precision.⁵ Trajectories that are close to each other near the fixed point can vastly differ in their IR physics. In practice, this issue is realized in different ways within the sub-landscape attached to FP2. This is because the above-mentioned boundary trajectories are separatrices that connect FP2 to FP1 and MFP, respectively.⁶ As a consequence, going towards the separatrix to FP1, the Wilson coefficients approach those of FP1. On the other hand, approaching MFP, the Wilson coefficients become larger and larger. The reason is that one approaches the separatrix between MFP and the GFP. For this trajectory, Newton’s coupling vanishes identically, so our definition of Wilson coefficients is ill-defined and only their ratios are still well-defined, cf. [Section 3.7](#).

With this remark out of the way, let us discuss the sub-landscape of FP2. In [Figure 4](#) we show different views on the Wilson coefficients within this sub-landscape (purple dots), as well as the EFT generated by FP1 (red dot). The overall geometry resembles that of a stretched-out candy cane: most of this sub-landscape is approximated by a straight line (the extended “strabe”). At one end, this extended strabe terminates at the sub-landscape of MFP, which we will discuss in the next subsection. At the other end, there is a small curved part (the “warble”) that connects it to the sub-landscape from FP1, and gives the characteristic candy cane shape.

⁵Specifically, a working precision of 32 digits was required for our data points when using Mathematica’s NDSolve routine. We then chose initial conditions on a small circle about FP2 within its critical hypersurface, parameterized by an angle. We picked one specific trajectory that is well within the sub-landscape. From there, we changed the angle by a step of $\pi/10$. If the successive trajectory is still flowing into the GFP, we continue the procedure by changing the angle by the same amount, otherwise, we discard the trajectory, half the step size, and compute the next trajectory. We repeated this procedure until the step size fell below $10^{-18}\pi$. Finally, we added some additional trajectories to improve the density of data points in the sub-landscape.

⁶This means that the part of theory space that is both UV-complete and connected to the GFP in the IR looks very similar to that of the system of a shift-symmetric scalar field coupled to gravity in the same order of the derivative expansion, see [\[70\]](#).

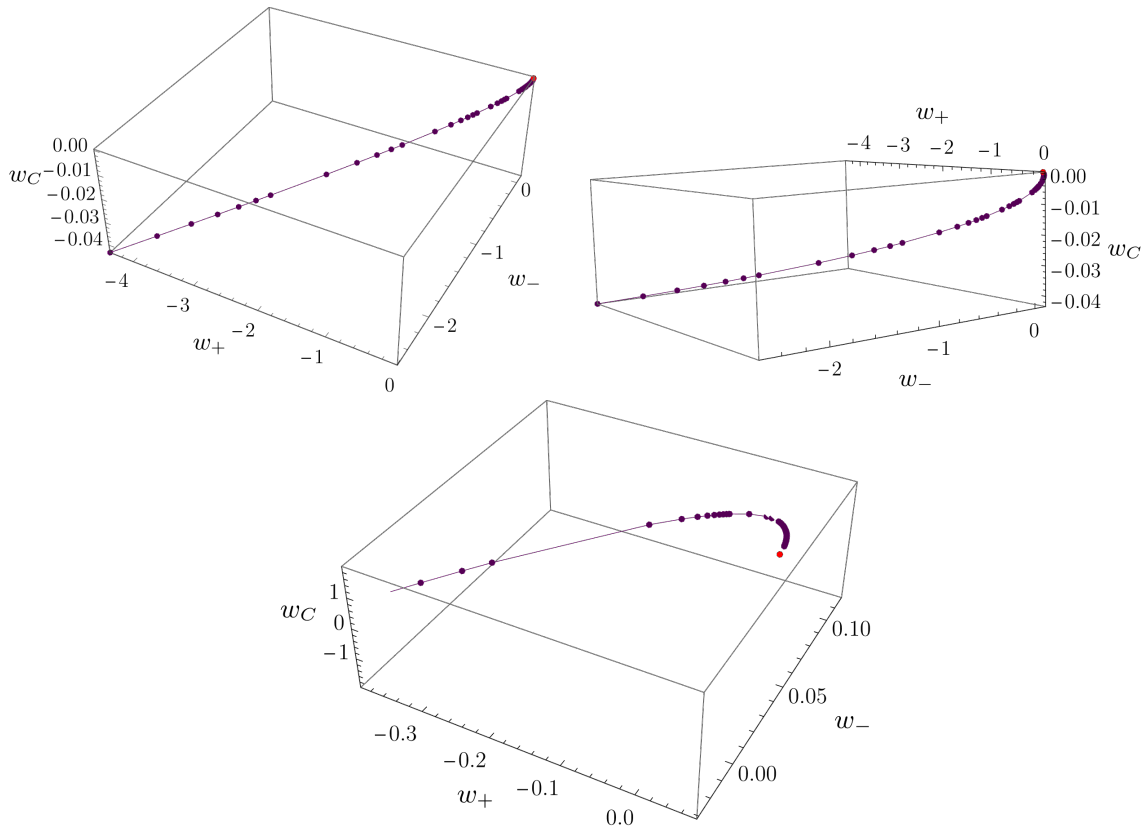


Figure 4. Different views and zooms on the AS landscape, in the space of dimensionless Wilson coefficients $\{w_+, w_-, w_C\}$. The dots denote the Wilson coefficients computed as the IR limit of a sample of asymptotically safe RG trajectories. The purple dots are the IR coefficients arising from FP2, whilst the red one is the sub-landscape stemming from FP1. The line connecting the points is an interpolating function. The overall landscape, given by the union of the sub-landscapes from FP1 and FP2, is approximately a straight line. The line however bends in the proximity of the FP2-landscape, forming a tiny “candy cane” which continuously connects the two sub-landscapes. Moreover, the entire landscape falls approximately onto a plane. Both the near-flatness, already encountered in [25], and the contiguity of the sub-landscapes are non-trivial features.

A thorough analysis of our data points shows that the extended strabe part of the sub-landscape can be approximated by a square root plus linear fit in the $\{w_+, w_-\}$ -plane, and by a quadratic fit along the w_C -direction.⁷ Concretely, fitting the 10 data points furthest away from the warble region, we find

$$w_- \approx 0.8022w_+ + 0.4353\sqrt{-w_+} + 0.03453, \quad (3.15)$$

and

$$\begin{aligned} w_+ &\approx -1666w_C^2 + 32.78w_C + 0.1566, \\ w_- &\approx -1359w_C^2 + 5.930w_C + 0.2341. \end{aligned} \quad (3.16)$$

⁷The form of these functions was selected by the fact that they fit large parts of the sub-landscape, significantly beyond the selection of data points used to obtain them.

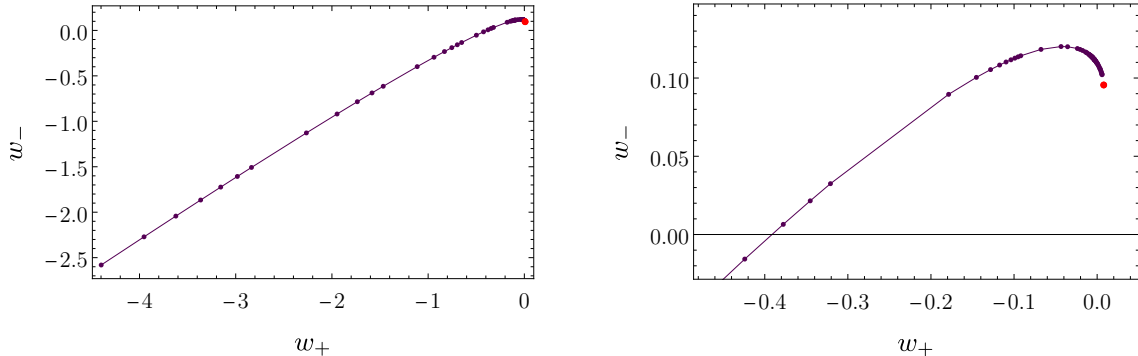


Figure 5. Projection of the AS landscape onto the bidimensional theory space $\{w_+, w_-\}$. In this plane the landscape preserves the characteristic “candy cane” shape. This is because the third Wilson coefficient varies very weakly across the entire landscape, $w_C \in [-0.043, 0.00026]$. As in Figure 4, purple dots are EFTs coming from FP2, whereas the red dot is the only EFT associated with FP1.

These fits are valid in the limit of large Wilson coefficients, i.e. as $w_{\pm, C} \rightarrow -\infty$, so that, to leading order, the extended strabe is a straight line in $\{w_{\pm}, w_C^2\}$. The rather large coefficients in the quadratic fits are entirely due to the fact that w_C is much smaller than w_{\pm} for our data points.

Remarkably, the *entire* sub-landscape originating from FP2 approximately lies on a plane described by

$$w_C = 0.0049155 + 0.038755w_+ - 0.047318w_- . \quad (3.17)$$

This is to mean that the candy cane is not bent significantly. For the points of the sub-landscape that were computed, the distance from this plane does not exceed 0.000057. Moreover, as w_C covers the small range $[-0.043, 0.00026]$ for our data points, the shape of the sub-landscape is approximately preserved when projecting it onto the bidimensional space $\{w_+, w_-\}$, see Figure 5. We remark once again that to determine all the above relations, we used $c_l = 16\pi$ to fix the logarithmic ambiguity in w_- .

Similar findings were also obtained in the first paper that computed a landscape from the RG flow of an asymptotically safe gravitational theory [25]. Concretely, in [25] the one-loop flow of quadratic gravity was investigated, and the resulting two-dimensional landscape was approximately a plane. This is an intriguing and highly non-trivial feature that deserves further investigation.

3.7 Sub-landscape from MFP

The fixed point MFP lies at $g = 0$ and thus it involves no gravity. Nonetheless, since it acts as one of the boundaries of the sub-landscape attached to FP2, we will briefly discuss the properties of its sub-landscape. First of all, since $g = 0$ at the fixed point, the separatrix between MFP and the GFP will have $g = 0$ at all scales, corresponding to a pure matter theory. This also entails that we have to use a different dimensionful coupling to set the scale. Second, and intriguingly, on this separatrix, we have an *exact* relation between g_+

and g_- ,

$$\frac{g_-}{g_+} = y \approx 0.826, \quad (3.18)$$

where y is the real root of the polynomial $(-73 + 131y - 59y^2 + 9y^3)$. This relation is fulfilled along the whole trajectory, which reduces the number of independent couplings to two. Stated differently, the Wilson coefficient resulting from the ratio g_-/g_+ is exactly y . Finally, since the fixed point has one relevant direction, the sub-landscape has only one non-trivial dimensionless Wilson coefficient. We find that

$$\frac{G_{CFF}}{\sqrt{-G_+}} \approx -0.0290. \quad (3.19)$$

We were able to compute its exact value in a closed form as well. Since only limited insights can be gained from it, we present it in (B.1) in Appendix B.

The importance of the relations (3.18) and (3.19) derives from the fact that, since the sub-landscape of FP2 is bounded by MFP, the relations must be fulfilled at the asymptotic end of the extended strabe. For our data points, this is not yet fulfilled — for the last data point, we find

$$\frac{g_-}{g_+} \approx 0.5997, \quad \frac{G_{CFF}}{\sqrt{-g_+}} \approx -0.02068. \quad (3.20)$$

This simply signals that our data at the open end of the strabe are not yet in the asymptotic regime, so they do not yet match the scaling of MFP. This emphasizes the aforementioned numerical challenge of mapping out the full sub-landscape of FP2.

We can nevertheless try to extract the exact limits (3.18) and (3.19) from our fits of the extended strabe, Eq. (3.15) and (3.16). While using the square root plus linear fit (3.15) yields $y \approx 0.8022$, employing the ratio of quadratic fits (3.16) and sending $w_C \rightarrow \infty$, we get $y \approx 0.816$. Both values are very close to the exact value. Likewise, using the quadratic fit for w_+ to compute the ratio (3.19), we obtain -0.0245 , which differs from the exact value by about 16%. Last but not least, we can also use the plane equation (3.17) to estimate (3.18), which is given by the ratio of the coefficients in front of w_{\pm} . From this, we get $y \approx 0.819$. This lends more support to the idea that the entire sub-landscape of FP2, including the asymptotic region close to MFP, indeed approximately lies on a plane.

4 Comparing the AS landscape with positivity, entropy, and weak gravity bounds

In terms of the dimensionless Wilson coefficients (3.4) and (3.6), the bounds introduced in Section 2 read

$$\begin{aligned} \text{Positivity bounds:} \quad & \mathcal{P}_1 = (16\pi G_N)^2 \Lambda^4 (2w_+ - w_- - |w_+|) > 0, \\ & \mathcal{P}_2 = 3w_+ - w_- - 2|w_C| > 0, \\ & \mathcal{P}_3 = w_+ - w_- > 0, \\ \text{Entropy bound:} \quad & \mathcal{P}_E = 8\pi G_N ((1 - \xi)^2 (3w_+ - w_-) \\ & \quad - 2(1 - \xi)(1 + 4\xi)w_C + 10\xi(1 + \xi)w_{\mathfrak{E}}) > 0, \\ \text{WGC:} \quad & \mathcal{P}_{\text{WGC}} = 8\pi G_N (3w_+ - w_- - 2w_C) > 0. \end{aligned} \quad (4.1)$$

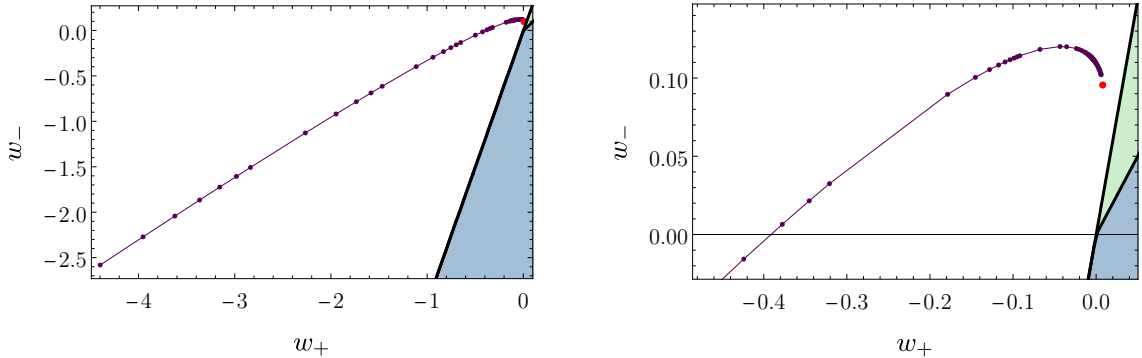


Figure 6. Comparison of the AS landscape with the combined positivity bounds (blue region) and WGC (green region). The two bounds partially overlap in this projection, with the first combined bounds being stronger than the second. The AS landscape lies outside of the region where the bounds are satisfied, and the violation is minimized by the sub-landscape identified by FP1 (red dot).

Insomuch as the only scale of our system is the Planck mass, we will set $\Lambda^2 = 1/(16\pi G_N)$, so that in the first bound all multiplicative factors disappear. At this point, it is important to highlight that while the individual Wilson coefficients w_i are neither gauge/parameterization independent, nor invariant under field redefinitions, the combinations of them appearing in scattering amplitudes and also in the \mathcal{P}_i are. In this section we will compare the above conditions with the AS landscape derived in the previous section. Our results are summarized in [Figure 6](#), [Figure 7](#), and [Figure 8](#).

The comparison of the global AS landscape of our system with the positivity bounds \mathcal{P}_i and the WGC condition \mathcal{P}_{WGC} shows that the arguments and conjectures in [\[53–55\]](#) are strictly realized within our system: Planck-scale suppressed violations of both positivity bounds and WGC occur across the entire landscape.⁸ This is visually evident in [Figure 6](#), where we show the projection of the AS landscape onto the plane $\{w_+, w_-\}$, together with the regions where positivity bounds and the WGC hold. We need to emphasize though that the theory space is parameterized via dimensionless Wilson coefficients so that all numbers are expressed in units of the Newton coupling, cf. [\(3.4\)](#) and [\(3.6\)](#).

Focusing on the violation of the WGC, the comparison of our results with that in [\[25\]](#) indicates the importance of the $U(1)$ sector and non-perturbativity in assessing the validity of the WGC. Indeed, [\[25\]](#) assumed electromagnetic duality and investigated the intersections between the AS landscape in one-loop quadratic gravity [\[78\]](#) and some swampland conjectures, including the WGC. The AS landscape of [\[25\]](#) was fully located inside the region $\mathcal{P}_{\text{WGC}} > 0$, so that the WGC was strictly valid throughout the landscape. The deviation of our result from that in [\[25\]](#) is to be attributed to several factors, from the improved computational setup (full-fledged FRG versus perturbative computation), to the inclusion of the $U(1)$ sector with essential couplings only, and the different universality class of the

⁸Whether positivity bounds are strictly fulfilled in some parts of the landscape may also depend on the approximations employed and, in truncated systems, on the choice of gauge and parameterization to set up the flow [\[77\]](#).

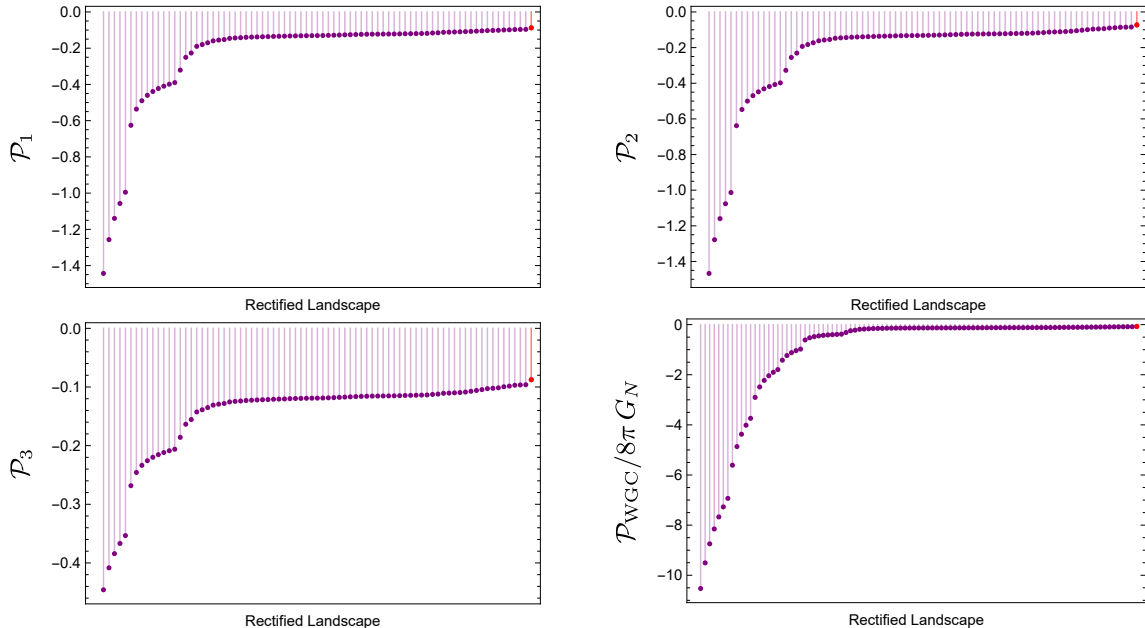


Figure 7. Planck-scale suppressed violations of positivity bounds and WGC on the rectified landscape, where data points are equidistant for better representation. As in other figures, the red dot corresponds to the single-point landscape generated by FP1, while the purple dots correspond to the EFTs in the sub-landscape identified by FP2. The plots show the dimensionless version of the violation for each \mathcal{P}_i , i.e., their deviation from positivity: the more negative, the larger the violation. As is apparent, the violation is minimized by the EFT associated with the most predictive fixed point (red dot) and gets large as one moves away from it along the sub-landscape of FP2.

UV fixed point [78].

The dimensionless amount of violation for each \mathcal{P}_i is shown in Figure 7. Each dot quantifies the dimensionless deviation from positivity of \mathcal{P}_i at a point of the rectified version of the landscape, where, aiming at a better visualization, all data points have been deformed to be equidistant. The more negative \mathcal{P}_i is, the larger the violation. In particular, the only EFT predicted by FP1 — denoted by a red dot — is the one where the violation is smallest. Moving along the landscape, and away from the red dot, the violation gets larger and larger.

Let us also briefly discuss the positivity bounds for the sub-landscape deriving from MFP. Due to the exact expressions for the Wilson coefficients, (3.18) and (3.19), and the fact that $g_+ < 0$ along the separatrix, we straightforwardly find that all positivity bounds are violated. Since this theory excludes gravitational fluctuations so that standard positivity bounds should apply, this entails that the UV completion of self-interacting photons provided by MFP is likely not unitary. From this perspective, AS might act as a unitarizer of the photonic theory through the fixed points FP1 and FP2.

So far we discussed the comparison of the AS landscape with the bounds $\mathcal{P}_{1,2,3}$ and \mathcal{P}_{WGC} . We now turn our attention to the family of entropy-based positivity bounds $\mathcal{P}_{\text{E}}(\xi)$. This constraint deserves a separate discussion because of its dependence on an external parameter, and, more notably, due to the appearance of the Euler Wilson coefficient w_{E} .

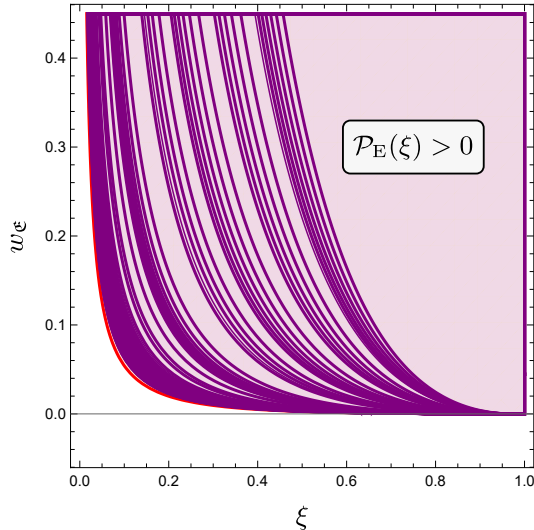


Figure 8. Constraints on the Euler Wilson coefficient resulting from the family of entropy bounds $\mathcal{P}_E(\xi)$. The bound depends on the point in the landscape: each of the purple lines corresponds to a point in the sub-landscape of FP2, whereas the red line is attached to the sub-landscape of FP1. In order to satisfy the bound, w_ϵ needs to be more positive for EFTs lying away from the single-point sub-landscape. Moreover, the bound is a function of the extremality parameter ξ . The smaller ξ is, the stronger the bound. For $\xi = 1$ the bound would imply the weak constraint $w_\epsilon \gtrsim 0$. Requiring that every bound in the family $\mathcal{P}_E(\xi)$ has to hold, implies that the strongest of them has to be satisfied. As is apparent from the figure, the strongest corresponds to the boundary case $\xi = 0$: on the one hand, for $\xi = 0$ the Euler Wilson coefficient drops out of $\mathcal{P}_E(\xi)$, and the resulting bound is the WGC. On the other hand, taking the limit $\xi \rightarrow 0^+$, independent of the specific RG trajectory the positivity of $\mathcal{P}_E(\xi)$ would imply $w_C \rightarrow +\infty$. The apparent mismatch is due to the weak violation of the WGC across the whole landscape.

As already discussed, the Euler coupling is special in purely field-theoretic setups, because its flow typically does not have non-trivial fixed points, and hence the corresponding Wilson coefficient w_ϵ is unconstrained. This atypical behavior and the lack of RG-induced constraints are generally not considered as issues, inasmuch w_ϵ does not enter on-shell quantities like scattering amplitudes. Yet, the Gauss-Bonnet term impacts off-shell quantities like the entropy [50, 79–83], even in four spacetime dimensions. It can consequently enter positivity bounds such as $\mathcal{P}_E(\xi)$. Such bounds can then result in constraints for the Euler Wilson coefficient, as shown in Figure 8. The individual constraints depend both on the extremality parameter ξ and on the point of the landscape. The bounds become stronger for points of the landscape further away from the single-point landscape and for smaller values of ξ . Thus, requiring that they all hold results in the requirement that the strongest of them is satisfied. In our case the strongest of the entropy bounds is realized in the limit $\xi \rightarrow 0^+$, in which case the Euler Wilson coefficient is constrained to be $w_C \rightarrow +\infty$. At the same time, setting $\xi = 0$ in the entropy positivity bounds $\mathcal{P}_E(\xi)$ yields the WGC and decouples the Euler Wilson coefficient. This discontinuity is due to the slight violation of the WGC, since if \mathcal{P}_{WGC} were positive, the limit $\xi \rightarrow 0^+$ would have implied $w_C > -\infty$.

instead, i.e., the absence of a bound.

Once again, this result is to be contrasted with the conclusions drawn in [25]. The use of a one-loop approximation in pure quadratic gravity has the effect of generating a fixed point for the Euler coupling, which is thus constrained to be positive in the landscape. In [25] this entailed the possibility of testing the validity of the entropy bounds $\mathcal{P}_E(\xi)$ within the AS landscape, in the Stelle universality class [78].

Overall, our results point to an intriguing lesson on the role of the Euler coupling in AS. Wilson coefficients associated with boundaries or spacetime topology, like the Euler coupling in our case, remain unbounded by the RG flow. Conditions like the entropy bounds $\mathcal{P}_E(\xi) > 0$ thus turn into constraints for these couplings. Predictivity thus hinges on a better understanding of the role of boundaries in AS, and perhaps the necessity of relating bulk and boundary Wilson coefficients via an AS version of the holographic principle.

5 Positivity bounds and WGC beyond Wilson coefficients: flowing conditions

Motivated by the cases of Ward identities [84] and the C -theorem [85], in this section we take a more general perspective, and ask the question whether positivity bounds and the WGC should hold at any FRG scales $k \geq 0$, or if they only apply to fully renormalized quantities. Along these lines, there are several questions about the validity of positivity and WGC along the flow: what is the relation between their realization along a given RG trajectory at finite k , and at its IR endpoint, i.e., in the limit $k \rightarrow 0$? Is it true that if positivity bounds are fulfilled/violated at the fixed point, they are also fulfilled/violated across the corresponding landscape?

While we will not try to prove any general statements, we will investigate the questions above for a sample of UV-complete trajectories that flow into the GFP in the IR. To this end, we investigate a “flowing” version of Wilson coefficients, defined by removing the $k \rightarrow 0$ -limit in the original definitions, (3.4) and (3.6), but still subtracting the logarithm along the whole flow as in (3.11c). We then insert these into the positivity bounds \mathcal{P}_i and study them as a function of k .

As a first example, we consider the flowing conditions for the separatrix between FP1 and the GFP. For this trajectory, $g_+ > 0$ and $g_{CF} > 0$, so that $\mathcal{P}_1 \equiv \mathcal{P}_3$ and $\mathcal{P}_2 \equiv \mathcal{P}_{WGC}/8\pi G_N$, and we are left with two independent bounds. As shown in Figure 9, in this case the positivity bounds are (Planck-scale) violated along the entire flow.

A second set of examples can be extracted from the flow emanating from FP2. Trajectories originating at FP2 start out with a stronger violation of the flowing positivity bounds than the trajectory starting at FP1. The flow then behaves differently depending on its specific initial conditions: for trajectories ending up in the warble part of the landscape, the violation decreases, and approaches that of the FP1-GFP separatrix. Near the crossover between warble and extended strabe, the violation stays approximately constant along the flow. Finally, in the extended strabe region, the violation increases along the flow. For these trajectories, g_+ and g_{CF} can be negative along the flow, so we do not necessarily

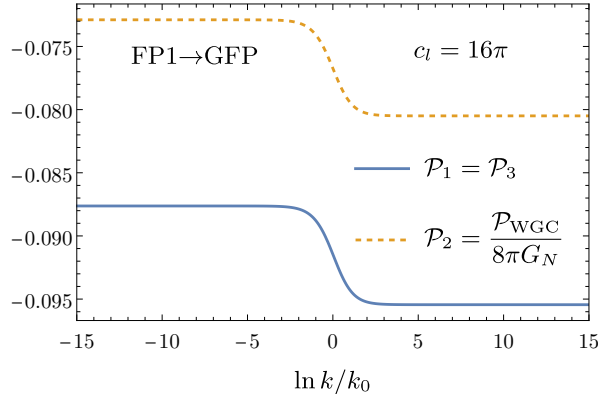


Figure 9. “Flowing” positivity bounds along the separatrix from FP1 to the GFP. We subtracted the logarithm in g_- along the whole flow with $c_l = 16\pi$. On this trajectory, $g_+ > 0$ and $g_{CFF} > 0$, so that $\mathcal{P}_1 = \mathcal{P}_3$ and $\mathcal{P}_2 = \mathcal{P}_{WGC}/8\pi G_N$. The two independent bounds $\mathcal{P}_1 > 0$ and $\mathcal{P}_2 > 0$ are violated along the entire flow, and the violation is an $\mathcal{O}(1)$ number in Planck units.

have a degeneracy of the positivity bounds as for the separatrix between FP1 and the GFP. In [Figure 10](#) we show these different behaviors.

In summary, in our system it is indeed true that the positivity bounds are Planck-scale violated along the whole flow for all trajectories that are UV-complete and end up in the GFP in the IR. This behavior would support the idea that a relationship exists between the fulfillment/violation of positivity bounds at non-zero k (including at the fixed point) and in the limit $k \rightarrow 0$, where all quantum fluctuations are integrated out. While we refrain from drawing conclusions from these few examples, the above behavior once again emphasizes that FP1 comes with the least amount of violation of the bounds, even along the flow connecting it to the IR.

6 Summary and conclusions

In this work, we computed the landscape of EFTs stemming from UV-complete (in particular, asymptotically safe) photon-graviton flows, and confronted it with entropy-based bounds that include the WGC as a particular case [\[50\]](#), and, for the first time, with positivity bounds [\[48, 49\]](#). The key idea is to generalize the notion of string landscape, which emerged within the swampland program [\[24, 34\]](#), to other approaches to QG and in particular to AS [\[25\]](#). This has the ultimate scope of identifying the intersections of QG landscapes, potentially highlighting connections between different approaches [\[27, 29, 30\]](#), systematically testing their consistency with bounds stemming from EFT [\[33\]](#), and assessing the validity of swampland conjectures beyond ST, especially in the light of the String Lamppost Principle [\[31, 32\]](#).

As a first step in this endeavor, we focused on a gravitational system non-minimally coupled to an Abelian gauge field in four spacetime dimensions. Our dynamics include (essential [\[86\]](#)) operators up to the fourth order in a derivative expansion, totaling five interaction couplings. Within this setup, we found that the beta functions provide two

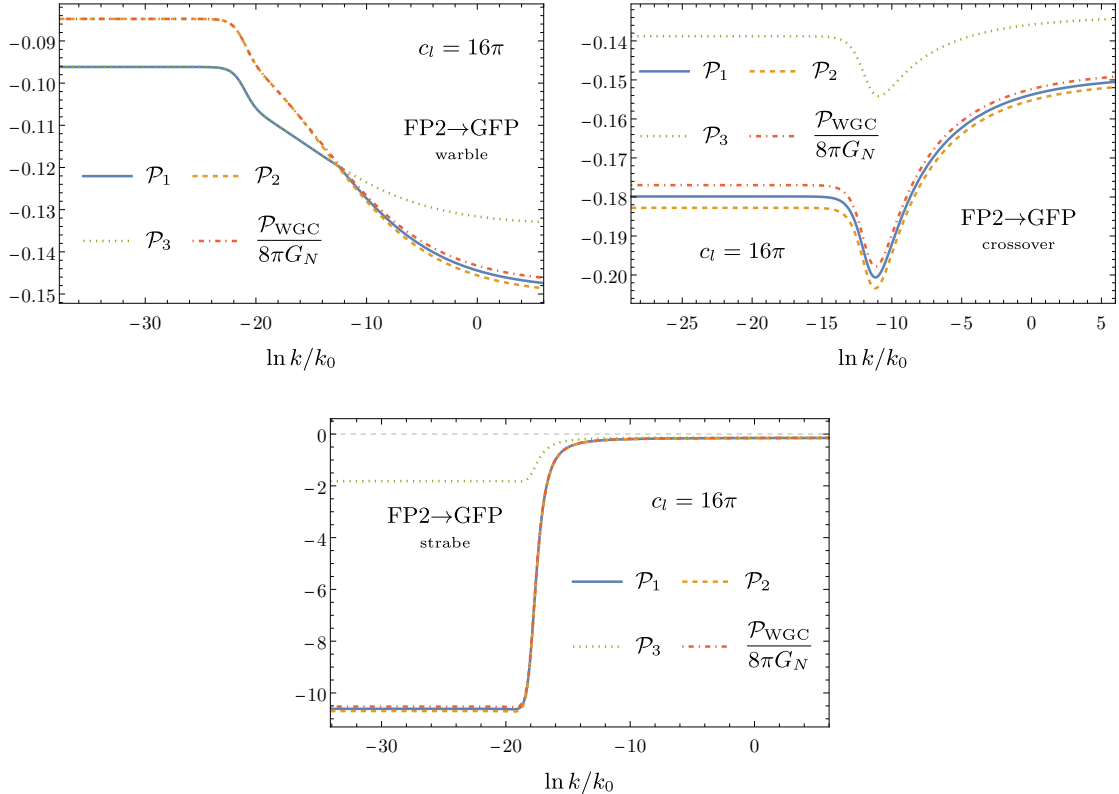


Figure 10. “Flowing” positivity bounds for three different trajectories emanating from FP2 and reaching three different parts of the candy cane: close to the separatrix to FP1 (warble), close to the separatrix to MFP (extended strabe), and in the crossover regime. We subtracted the logarithm in g_- along the whole flow with $c_l = 16\pi$. All trajectories display a violation of all positivity bounds along the entire flow. The violation becomes larger from the warble towards the extended strabe region, eventually surpassing an $\mathcal{O}(1)$ amount.

gravitational fixed points that can serve as UV-completion of the coupled theory, see [Table 1](#). The first has only one relevant direction, whose corresponding free parameter sets the scale of QG and the unit with respect to which all other dimensionful quantities are measured. The ensuing sub-landscape is zero-dimensional, namely, it is a single point in the space of dimensionless Wilson coefficients. The second fixed point has two relevant parameters. Given that one of them sets the unit mass scale, its corresponding sub-landscape is a line in the shape of a stretched-out candy cane, see [Figure 4](#). The tip of its small hook (the “warble”) meets the sub-landscape point of the first fixed point, so that the two sub-landscapes are continuously connected. A large part of the whole landscape is nearly a straight line (the extended “strabe”), whose other end is connected to a pure photon fixed point. Intriguingly, the entire landscape can be approximately embedded into a plane — a non-trivial feature that has been observed before [\[25\]](#). Whether this is a coincidence or a universal feature of AS is unclear, and deserves further systematic investigations.

We then confronted the set of Wilson coefficients within the AS landscape with a collection of bounds stemming from different considerations, from positivity bounds motivated

by unitarity and causality properties of scattering amplitudes [48, 49], to a family of constraints based on the positivity of the entropy of black holes under the addition of higher order curvature operators. The latter also includes (one form of the) the electric WGC as a particular case [50]. While positivity bounds are typically derived by excluding graviton fluctuations, they may nevertheless indicate whether parts of the landscape violate either unitarity or assumptions like low spin dominance or Regge limit, which are key in the derivation of positivity bounds [54]. The motivation for this is the fact that violations of such bounds are generally expected upon the inclusion of gravitational fluctuations [53, 55, 63], and are Planck-scale suppressed as long as the coefficients are of order one, cf. Eq. (2.7). Similar considerations also apply to the violation of the WGC, where the allowed amount of negativity in the presence of a new physics scale was estimated in [55].

We found that both the positivity bounds of [48, 49] and the WGC are violated across the entire AS landscape, but that indeed for large parts of it, the violation is Planck-scale suppressed. This is consistent with general expectations [53, 55, 63]. At the sub-landscape point of the most predictive fixed point, the violation is maximally suppressed. The violation slightly increases along the warble part of the other sub-landscape. The further along the extended strabe one progresses, the larger the coefficients of the violations become. This behavior is not surprising, since in the asymptotic limit of the extended strabe, the pure photon (i.e., gravity-free) fixed point [87] is approached, where standard positivity bounds are violated. A more thorough investigation, along the lines of [88, 89], is needed to understand the properties of this fixed point and its unitarity further. We can also turn our perspective around: starting from this non-unitary self-interacting photon theory, Asymptotically Safe Gravity acts as a “unitarizer” since the addition of gravity and the requirement of maximizing predictivity bring the theory closer to fulfilling standard unitarity bounds.⁹ Indeed, as already highlighted, the most predictive theory (the single-point landscape) is the one minimizing the already Planck-scale-suppressed violations of positivity bounds, suggesting an ideal scenario which combines high predictivity with the eventual fulfillment of modified positivity bounds.

Along with positivity bounds, we also investigated a family of entropy-based positivity constraints, which include the WGC as a particular case [50]. Since these are off-shell bounds, they can (and do) include the coupling of the topological Euler term. Since the Gauss-Bonnet operator is a topological invariant, its coupling does not appear in any beta function, and thus generically does not have a fixed point [57, 58]. As a consequence, the landscape-value of the Euler coupling is unconstrained, and within the current setup and state-of-the-art, such entropy-based bounds put constraints on the Euler coupling, rather than being a direct test of AS.

Our results are based on a setup that should be improved in future work. First, our computations were performed in Euclidean signature, which made a Wick rotation necessary in order to relate the resulting AS landscape to entropy and positivity bounds. Recent progress in the field [17] has shown that the spacetime signature does not strongly impact

⁹This goes along with the idea that AS provides an avenue to solve the triviality problem of the $U(1)$ sector [90].

the flow, but it would be noteworthy to investigate whether this statement applies to the whole AS landscape. Second, approximations had to be made, in our case by truncating the effective action to fourth order in derivatives. It is conceivable that improved approximations [71] and a better understanding of gauge and parameterization dependence of the flow [91] could push the most predictive fixed point into a regime where standard positivity bounds are satisfied. Third, to achieve a more realistic description [23], an extended field content has to be included, which would contribute to the relevant Wilson coefficients. Last but not least, grounded on the discussion above, the role of the Euler coupling has to be clarified within AS: it has to be understood what AS can, or cannot say, about black hole entropy (along the lines of [83, 92]) and, more generally, if a relation exists between bulk and boundary couplings, which could enhance the predictive power of off-shell quantities in this approach.

Finally, what would it mean if all these shortcomings were addressed, and AS would still violate positivity bounds? There are different options in this case. The violation could simply indicate that AS does not fulfill at least one of the assumptions underlying the derivation of positivity bounds. Potential candidates for these include the violation of microcausality or locality, which is not unrealistic for a theory of QG. Alternatively, as mentioned earlier, the violation could be related to the low-spin dominance hypothesis not being realized, which is assumed for the derivation, but whose violation would not pose any obvious problems for QG. Additionally, a violation could also mean that the existence of a UV fixed point is not enough to obtain a unitary and causal theory. Indications for the latter were indeed found in the study of general non-perturbative scattering amplitudes [93]. All these possibilities point to two key aspects within this endeavor: on the EFT side, the necessity of understanding positivity bounds in the presence of gravitational fluctuations and beyond perturbative settings [56, 94, 95], with an improved understanding of the relation between violations and their sources. On the AS side, the importance of mapping the UV features of the AS fixed point to the IR properties of the corresponding landscape [25].

Acknowledgments

The authors would like to thank I. Basile, G. N. Remmen, C. de Rham, A. Tokareva, and A. Tolley for interesting discussions, and I. Basile for feedback on the manuscript. The research of A.P. is supported by a research grant (VIL60819) from VILLUM FONDEN. A.P. also acknowledges support by Perimeter Institute for Theoretical Physics during the development of this project. B.K. is grateful for the hospitality of Perimeter Institute where part of this work was carried out. Research at Perimeter Institute is supported in part by the Government of Canada through the Department of Innovation, Science and Economic Development and by the Province of Ontario through the Ministry of Colleges and Universities. The research of B.K. is supported by Nordita. A.P. is grateful to Nordita for support within the “Nordita Distinguished Visitors” program and for hospitality during the early stages of this work. Nordita is supported in part by NordForsk.

A Photon-graviton flows: setup and definitions

In this section, we review the framework of the FRG and briefly discuss its modifications when accounting for field redefinitions. Afterward, we motivate our ansatz (3.1) for the effective action, and give details on the chosen gauge fixing and regularization.

A.1 The Functional Renormalization Group

The FRG is a powerful theoretical framework that is extensively employed in condensed matter physics, quantum field theory, and beyond [60], as a prescription to evaluate the path integral and to investigate non-perturbative RG flows. Unlike traditional RG techniques, which focus on coarse-graining in momentum space, the FRG operates directly in the space of actions, offering a more versatile approach to study strongly interacting systems. Specifically, the FRG is based on a modification of the effective action by an IR regulator. The latter has the dual scope of providing a prescription to regularize the path integral and of implementing the Wilsonian idea of shell-by-shell integration of modes. With the regularization implemented, the path integral can be translated into an exact functional differential equation [96–98] for the modified effective action Γ_k ,

$$k\partial_k\Gamma_k = \frac{1}{2}\text{STr} \left\{ \left(\Gamma_k^{(2)} + \mathfrak{R}_k \right)^{-1} k\partial_k \mathfrak{R}_k \right\}. \quad (\text{A.1})$$

Here, $\Gamma_k^{(2)}$ is the second functional derivative of Γ_k with respect to the underlying fields, \mathfrak{R}_k is the regulator implementing the successive mode integration, and STr denotes a so-called “super-trace”, i.e. a sum over discrete indices and an integration over continuous variables, together with a minus sign for Grassmann-valued fields. By construction, in the limit $k \rightarrow 0$, we obtain the fully renormalized couplings and thus the corresponding Wilson coefficients.

An essential ingredient for theories with gauge symmetries like gravity is the background field formalism. To be able to define a gauge fixing and a regularization, it is necessary to split the metric g into an arbitrary background metric \bar{g} and fluctuations h about it,

$$g_{\mu\nu} = \bar{g}_{\mu\nu} + h_{\mu\nu}. \quad (\text{A.2})$$

In our computation, we furthermore restrict ourselves to the so-called background field approximation, where we set h to zero after having computed the two-point function $\Gamma_k^{(2)}$. For an overview of how to go beyond this, see e.g. [10, 99].

Our focus in this work is to compute the landscape of AS, and to evaluate IR constraints like positivity bounds. To simplify the technical setup, we implement field redefinitions to eliminate as many inessential running couplings [86] as possible. One minimal way of eliminating inessential couplings within the FRG has been introduced in [64], and is based on an appropriate k -dependent field redefinition at the level of the flow equation,

$$k\partial_k\Gamma_k + \Psi_k \Gamma_k^{(1)} = \frac{1}{2}\text{STr} \left\{ \left(\Gamma_k^{(2)} + \mathfrak{R}_k \right)^{-1} \left[k\partial_k + 2\Psi_k^{(1)} \right] \mathfrak{R}_k \right\}. \quad (\text{A.3})$$

This equation is based on a more general flow equation [100, 101], see [102, 103] for earlier applications. The modification resides in the RG kernel Ψ_k , which is the expectation value of the flow of the redefined microscopic field. In practice, an ansatz is chosen for Ψ_k , and in principle one has to check a posteriori whether this indeed corresponds to a well-defined field redefinition. Couplings that can be removed by Ψ_k are inessential, whereas all other couplings are the essential ones. The latter are also the only ones that can appear in observables like scattering amplitudes. The “essential” version of the FRG flow has been applied widely, see e.g. [19, 65, 70, 71, 104]. A critical discussion is given in [105].

A.2 Action, gauge fixing, regularization and field redefinitions

The flow equations (A.1) and (A.3) can usually not be solved exactly, i.e. for a generic Γ_k . The standard approach is to specify symmetry, field content, an ordering criterion for the operators, and a truncation order that is typically dictated by the computational limitations. The elimination of inessential couplings via the flow equation (A.3) is a powerful instrument to push both truncation order and number of non-minimally coupled fields beyond previous computational limitations. In our work, we employ a derivative expansion of the effective action, and we include all essential couplings in QG coupled to an Abelian gauge field with up to four derivatives. To this order, the essential part of the action reads

$$\begin{aligned} \Gamma_k = & \int d^4x \sqrt{g} \left[\frac{1}{16\pi G_N} (2\Lambda - R) + G_{\mathfrak{E}} \mathfrak{E} \right] \\ & + \int d^4x \sqrt{g} \left[\mathcal{F}_2 + G_{\mathcal{F}_2} (\mathcal{F}_2)^2 + G_{\mathcal{F}_4} \mathcal{F}_4 + G_{CFF} C^{\mu\nu\rho\sigma} F_{\mu\nu} F_{\rho\sigma} \right], \end{aligned} \quad (\text{A.4})$$

where, as usual, all couplings depend on the scale k , and the operators \mathcal{F}_2 , \mathcal{F}_4 , and \mathfrak{E} are those introduced in (1.2). Compared to the action in (3.1), the above effective action includes a cosmological constant. Although the latter is the lowest-order operator in a derivative expansion, observationally $\Lambda G_N \ll 1$, and thus, in a first approximation, we will consider $\Lambda = 0$ in the limit $k \rightarrow 0$. Based on these considerations, and following the argumentation of [65], we use the field redefinition to fix λ to be proportional to g , entailing a vanishing dimensionful cosmological constant for the effective action(1.1).

Since our system admits gauge symmetries, the effective action has to be complemented by a gauge fixing term. We employ the harmonic gauge in both sectors, so that

$$\Gamma_{\text{gf}} = \int d^4x \sqrt{\bar{g}} \left[\frac{1}{32\pi G_N} \left(\bar{D}^\alpha h_{\mu\alpha} - \frac{1}{2} \bar{D}_\mu h \right) \left(\bar{D}_\beta h^{\mu\beta} - \frac{1}{2} \bar{D}^\mu h \right) + \frac{1}{2} (\bar{D}^\mu a_\mu)^2 \right]. \quad (\text{A.5})$$

This gives rise to a Faddeev-Popov ghost action of the form

$$\Gamma_c = \frac{1}{\sqrt{G_N}} \int d^4x \sqrt{\bar{g}} \bar{c}_\mu [\bar{\Delta} \delta^\mu{}_\nu - \bar{R}^\mu{}_\nu] c^\nu + \int d^4x \sqrt{\bar{g}} \bar{b} \bar{\Delta} b, \quad (\text{A.6})$$

where $\bar{\Delta} = -\bar{D}^2$. The next ingredient that we need to compute the RG flow is the regulator. For this, we follow the argumentation of [70] and introduce the “natural” endomorphisms

in all sectors. This entails

$$\mathfrak{R}_k^h = \frac{1}{32\pi G_N} [\mathcal{R}(\bar{\Delta}_2)\Pi^{\text{TL}} - \mathcal{R}(\bar{\Delta})\Pi^{\text{Tr}}] , \quad (\text{A.7})$$

$$\mathfrak{R}_k^a = \mathcal{R}(\bar{\Delta}_a)\mathbb{1} , \quad (\text{A.8})$$

$$\mathfrak{R}_k^c = \mathcal{R}(\bar{\Delta}_c)\mathbb{1} , \quad (\text{A.9})$$

$$\mathfrak{R}_k^b = \mathcal{R}(\bar{\Delta}) . \quad (\text{A.10})$$

We have identified all regulator shapes for simplicity, and $\Pi^{\text{TL,Tr}}$ denote the traceless and trace projectors, respectively. Eventually, we employed the Litim regulator [106],

$$\mathcal{R}(x) = (k^2 - x)\theta(1 - x/k^2) . \quad (\text{A.11})$$

The operators used in the regulators read

$$\bar{\Delta}_2^{\mu\nu}{}_{\rho\sigma} = \left(\bar{\Delta} + \frac{2}{3}\bar{R} \right) \Pi^{\text{TL}\mu\nu}{}_{\rho\sigma} - 2\bar{C}^{\mu\rho}{}_{\nu\sigma} , \quad \bar{\Delta}_a{}^\mu{}_\nu = \bar{\Delta}\delta^\mu{}_\nu + \bar{R}^\mu{}_\nu , \quad \bar{\Delta}_c{}^\mu{}_\nu = \bar{\Delta}\delta^\mu{}_\nu - \bar{R}^\mu{}_\nu . \quad (\text{A.12})$$

The final ingredient for the RG flow of essential couplings is the specification of the RG kernel. Since we have two different fields, we can perform a field redefinition in the combined field space. At the order that we consider here, the most general corresponding RG kernels are

$$\begin{aligned} \Psi_{\mu\nu}^g &= \gamma_g g_{\mu\nu} + \gamma_R R g_{\mu\nu} + \gamma_S S_{\mu\nu} + \gamma_{\mathcal{F}_2} \mathcal{F}_2 g_{\mu\nu} + \gamma_{F^2}^{\text{TL}} (F_{\mu\alpha} F^\alpha{}_\nu + \mathcal{F}_2 g_{\mu\nu}) , \\ \Psi_\mu^a &= \gamma_a a_\mu + \gamma_{DF} D^\alpha F_{\mu\alpha} . \end{aligned} \quad (\text{A.13})$$

Here, we set up the metric RG kernel in a way to split it into trace and traceless parts, which disentangles the equations for the gamma functions maximally. To read off the beta and gamma functions, we complete the monomials in our action by the following invariants to form a basis:

$$R^2 , \quad S^{\mu\nu} S_{\mu\nu} , \quad F^{\mu\nu} \Delta F_{\mu\nu} , \quad R F^{\mu\nu} F_{\mu\nu} , \quad S^{\mu\nu} F_{\mu\alpha} F^\alpha{}_\nu . \quad (\text{A.14})$$

This completes the discussion of the setup. With these ingredients as starting point, the computation of RG flow has been performed with the help of the Mathematica package xAct [66–68] and a well-tested code [69–71]. The complete set of beta functions can be found in the accompanying notebook [72].

B Analytic Wilson coefficient in the pure matter theory

The analytic expression for the Wilson coefficient given in (3.19) is

$$\frac{G_{CFF}}{\sqrt{-G_+}} = -\sqrt{\frac{a_1}{\pi}} \frac{\Gamma(a_2)}{\Gamma(a_2 + \frac{1}{2})} \left[{}_2F_1\left(\frac{1}{2}, a_3, a_2 + \frac{1}{2} \middle| z\right) + a_4 {}_2F_1\left(\frac{1}{2}, a_3 + 1, a_2 + \frac{3}{2} \middle| z\right) \right] , \quad (\text{B.1})$$

where the numbers $a_{1,2,3,4}$ and z are roots of low-order polynomials that can be obtained as follows. The number a_1 is the real root of the polynomial

$$\begin{aligned} & 10793861 + 18949368102912x + 30552729884565700608x^2 \\ & - 1619614712642678776922112x^3 - 9100076856720841554681397248x^4 \\ & - 16902672123436474482083424632832x^5 + 3161447767348821628323748676370432x^6 \end{aligned} \quad (\text{B.2})$$

near the point

$$a_1 \approx 0.0000177. \quad (\text{B.3})$$

For $a_{2,3}$, we define the polynomial

$$\begin{aligned} & 413044310016 - 10879053926400x \\ & + 158650842599040x^2 - 1291967177365900x^3 \\ & + 4894717105389125x^4 - 8447086388113750x^5 + 5813784153762500x^6. \end{aligned} \quad (\text{B.4})$$

The number a_2 is then the real root of this polynomial near

$$a_2 \approx 0.113, \quad (\text{B.5})$$

whereas a_3 is minus the root of the other real root of this polynomial,

$$a_3 \approx -0.313. \quad (\text{B.6})$$

Next, the number a_4 is the real root of the polynomial

$$\begin{aligned} & 307642010808877056 + 179837560477922623488x \\ & + 48915980589977271545856x^2 + 5843687635359647850841088x^3 \\ & + 826964630953265786764096x^4 + 39539603437261811380528x^5 \\ & + 646308740102823594591x^6 \end{aligned} \quad (\text{B.7})$$

near the point

$$a_4 \approx -0.00395. \quad (\text{B.8})$$

Finally, the number z is the real root of the polynomial

$$\begin{aligned} & 5967 - 7673436x + 3561700932x^2 - 554287751986x^3 \\ & + 3561700932x^4 - 7673436x^5 + 5967x^6 \end{aligned} \quad (\text{B.9})$$

close to

$$z \approx 0.00303. \quad (\text{B.10})$$

References

- [1] T. Appelquist and J. Carazzone, *Infrared Singularities and Massive Fields*, *Phys. Rev. D* **11** (1975) 2856.

- [2] A. Bonanno, A. Eichhorn, H. Gies, J.M. Pawłowski, R. Percacci, M. Reuter et al., *Critical reflections on asymptotically safe gravity*, *Front. in Phys.* **8** (2020) 269 [2004.06810].
- [3] B. Knorr, C. Ripken and F. Saueressig, *Form Factors in Asymptotically Safe Quantum Gravity*, [2210.16072](#).
- [4] A. Eichhorn and M. Schiffer, *Asymptotic safety of gravity with matter*, [2212.07456](#).
- [5] T.R. Morris and D. Stulga, *The functional $f(R)$ approximation*, [2210.11356](#).
- [6] R. Martini, G.P. Vacca and O. Zanusso, *Perturbative approaches to non-perturbative quantum gravity*, [2210.13910](#).
- [7] C. Wetterich, *Quantum gravity and scale symmetry in cosmology*, [2211.03596](#).
- [8] A. Platania, *Black Holes in Asymptotically Safe Gravity*, [2302.04272](#).
- [9] F. Saueressig, *The Functional Renormalization Group in Quantum Gravity*, [2302.14152](#).
- [10] J.M. Pawłowski and M. Reichert, *Quantum Gravity from dynamical metric fluctuations*, [2309.10785](#).
- [11] A. Bonanno, *Asymptotic Safety and Cosmology*, in *Handbook of Quantum Gravity* (2024), [DOI](#).
- [12] M. Reuter, *Nonperturbative evolution equation for quantum gravity*, *Phys.Rev.* **D57** (1998) 971 [[hep-th/9605030](#)].
- [13] K. Falls, D.F. Litim, K. Nikolakopoulos and C. Rahmede, *Further evidence for asymptotic safety of quantum gravity*, *Phys. Rev.* **D93** (2016) 104022 [[1410.4815](#)].
- [14] H. Gies, B. Knorr, S. Lippoldt and F. Saueressig, *Gravitational Two-Loop Counterterm Is Asymptotically Safe*, *Phys. Rev. Lett.* **116** (2016) 211302 [[1601.01800](#)].
- [15] A. Platania and C. Wetterich, *Non-perturbative unitarity and fictitious ghosts in quantum gravity*, *Phys. Lett. B* **811** (2020) 135911 [[2009.06637](#)].
- [16] A. Bonanno, T. Denz, J.M. Pawłowski and M. Reichert, *Reconstructing the graviton*, *SciPost Phys.* **12** (2022) 001 [[2102.02217](#)].
- [17] J. Fehre, D.F. Litim, J.M. Pawłowski and M. Reichert, *Lorentzian Quantum Gravity and the Graviton Spectral Function*, *Phys. Rev. Lett.* **130** (2023) 081501 [[2111.13232](#)].
- [18] A. Platania, *Causality, unitarity and stability in quantum gravity: a non-perturbative perspective*, *JHEP* **09** (2022) 167 [[2206.04072](#)].
- [19] B. Knorr, *Momentum-dependent field redefinitions in Asymptotic Safety*, [2311.12097](#).
- [20] P. Donà, A. Eichhorn and R. Percacci, *Matter matters in asymptotically safe quantum gravity*, *Phys.Rev.* **D89** (2014) 084035 [[1311.2898](#)].
- [21] A. Eichhorn and A. Held, *Top mass from asymptotic safety*, *Phys. Lett.* **B777** (2018) 217 [[1707.01107](#)].
- [22] A. Eichhorn, *Status update: Asymptotically safe gravity-matter systems*, *Nuovo Cim. C* **45** (2022) 29 [[2201.11543](#)].
- [23] A. Pastor-Gutiérrez, J.M. Pawłowski and M. Reichert, *The Asymptotically Safe Standard Model: From quantum gravity to dynamical chiral symmetry breaking*, *SciPost Phys.* **15** (2023) 105 [[2207.09817](#)].
- [24] C. Vafa, *The String landscape and the swampland*, [hep-th/0509212](#).

- [25] I. Basile and A. Platania, *Asymptotic Safety: Swampland or Wonderland?*, *Universe* **7** (2021) 389 [2107.06897].
- [26] R. Percacci and G.P. Vacca, *Asymptotic Safety, Emergence and Minimal Length*, *Class. Quant. Grav.* **27** (2010) 245026 [1008.3621].
- [27] S. de Alwis, A. Eichhorn, A. Held, J.M. Pawłowski, M. Schiffer and F. Versteegen, *Asymptotic safety, string theory and the weak gravity conjecture*, *Phys. Lett. B* **798** (2019) 134991 [1907.07894].
- [28] A. Held, *Effective asymptotic safety and its predictive power: Gauge-Yukawa theories*, *Front. in Phys.* **8** (2020) 341 [2003.13642].
- [29] I. Basile and A. Platania, *Cosmological α' -corrections from the functional renormalization group*, *JHEP* **06** (2021) 045 [2101.02226].
- [30] I. Basile and A. Platania, *String tension between de Sitter vacua and curvature corrections*, *Phys. Rev. D* **104** (2021) L121901 [2103.06276].
- [31] V. Kumar and W. Taylor, *String Universality in Six Dimensions*, *Adv. Theor. Math. Phys.* **15** (2011) 325 [0906.0987].
- [32] M. Montero and C. Vafa, *Cobordism Conjecture, Anomalies, and the String Lamppost Principle*, *JHEP* **01** (2021) 063 [2008.11729].
- [33] C. de Rham, S. Kundu, M. Reece, A.J. Tolley and S.-Y. Zhou, *Snowmass White Paper: UV Constraints on IR Physics*, in *Snowmass 2021*, 3, 2022 [2203.06805].
- [34] E. Palti, *The Swampland: Introduction and Review*, *Fortsch. Phys.* **67** (2019) 1900037 [1903.06239].
- [35] P. Agrawal, G. Obied, P.J. Steinhardt and C. Vafa, *On the Cosmological Implications of the String Swampland*, *Phys. Lett. B* **784** (2018) 271 [1806.09718].
- [36] A. Bedroya, R. Brandenberger, M. Loverde and C. Vafa, *Trans-Planckian Censorship and Inflationary Cosmology*, *Phys. Rev. D* **101** (2020) 103502 [1909.11106].
- [37] C. Angelantonj, Q. Bonnefoy, C. Condeescu and E. Dudas, *String Defects, Supersymmetry and the Swampland*, *JHEP* **11** (2020) 125 [2007.12722].
- [38] E. Gonzalo, L.E. Ibáñez and I. Valenzuela, *AdS swampland conjectures and light fermions*, *Phys. Lett. B* **822** (2021) 136691 [2104.06415].
- [39] M. Graña and A. Herráez, *The Swampland Conjectures: A Bridge from Quantum Gravity to Particle Physics*, *Universe* **7** (2021) 273 [2107.00087].
- [40] L.A. Anchordoqui, I. Antoniadis and J. Cunat, *Dark dimension and the standard model landscape*, *Phys. Rev. D* **109** (2024) 016028 [2306.16491].
- [41] C. Vafa, *Swamplandish Unification of the Dark Sector*, 2402.00981.
- [42] B. Knorr, C. Ripken and F. Saueressig, *Form Factors in Quantum Gravity: Contrasting non-local, ghost-free gravity and Asymptotic Safety*, *Nuovo Cim. C* **45** (2022) 28 [2111.12365].
- [43] M. Montero and M. Tartaglia, *Exotic supergravities and the Swampland*, 2403.15535.
- [44] N. Arkani-Hamed, L. Motl, A. Nicolis and C. Vafa, *The String landscape, black holes and gravity as the weakest force*, *JHEP* **06** (2007) 060 [hep-th/0601001].

- [45] M. Montero, *A Holographic Derivation of the Weak Gravity Conjecture*, *JHEP* **03** (2019) 157 [[1812.03978](#)].
- [46] D. Harlow, B. Heidenreich, M. Reece and T. Rudelius, *Weak gravity conjecture*, *Rev. Mod. Phys.* **95** (2023) 035003 [[2201.08380](#)].
- [47] B. Heidenreich and M. Lotito, *Proving the Weak Gravity Conjecture in Perturbative String Theory, Part I: The Bosonic String*, [2401.14449](#).
- [48] B. Bellazzini, M. Lewandowski and J. Serra, *Positivity of Amplitudes, Weak Gravity Conjecture, and Modified Gravity*, *Phys. Rev. Lett.* **123** (2019) 251103 [[1902.03250](#)].
- [49] M. Carrillo González, C. de Rham, S. Jaitly, V. Pozsgay and A. Tokareva, *Positivity-causality competition: a road to ultimate EFT consistency constraints*, [2307.04784](#).
- [50] C. Cheung, J. Liu and G.N. Remmen, *Proof of the Weak Gravity Conjecture from Black Hole Entropy*, *JHEP* **10** (2018) 004 [[1801.08546](#)].
- [51] Y. Kats, L. Motl and M. Padi, *Higher-order corrections to mass-charge relation of extremal black holes*, *JHEP* **12** (2007) 068 [[hep-th/0606100](#)].
- [52] Y. Hamada, T. Noumi and G. Shiu, *Weak Gravity Conjecture from Unitarity and Causality*, *Phys. Rev. Lett.* **123** (2019) 051601 [[1810.03637](#)].
- [53] L. Alberte, C. de Rham, S. Jaitly and A.J. Tolley, *Positivity Bounds and the Massless Spin-2 Pole*, *Phys. Rev. D* **102** (2020) 125023 [[2007.12667](#)].
- [54] M. Herrero-Valea, R. Santos-Garcia and A. Tokareva, *Massless positivity in graviton exchange*, *Phys. Rev. D* **104** (2021) 085022 [[2011.11652](#)].
- [55] J. Henriksson, B. McPeak, F. Russo and A. Vichi, *Bounding violations of the weak gravity conjecture*, *JHEP* **08** (2022) 184 [[2203.08164](#)].
- [56] M. Herrero-Valea, A.S. Koshelev and A. Tokareva, *UV graviton scattering and positivity bounds from IR dispersion relations*, *Phys. Rev. D* **106** (2022) 105002 [[2205.13332](#)].
- [57] K. Falls, N. Ohta and R. Percacci, *Towards the determination of the dimension of the critical surface in asymptotically safe gravity*, *Phys. Lett. B* **810** (2020) 135773 [[2004.04126](#)].
- [58] B. Knorr, *The derivative expansion in asymptotically safe quantum gravity: general setup and quartic order*, *SciPost Phys. Core* **4** (2021) 20 [[2104.11336](#)].
- [59] M. Reuter and F. Saueressig, *Quantum Gravity and the Functional Renormalization Group*, Cambridge University Press (2019).
- [60] N. Dupuis, L. Canet, A. Eichhorn, W. Metzner, J.M. Pawłowski, M. Tissier et al., *The nonperturbative functional renormalization group and its applications*, *Physics Reports* (2020) [[2006.04853](#)].
- [61] S. Caron-Huot, D. Mazac, L. Rastelli and D. Simmons-Duffin, *Sharp boundaries for the swampland*, *JHEP* **07** (2021) 110 [[2102.08951](#)].
- [62] S. Caron-Huot, Y.-Z. Li, J. Parra-Martinez and D. Simmons-Duffin, *Causality constraints on corrections to Einstein gravity*, *JHEP* **05** (2023) 122 [[2201.06602](#)].
- [63] L. Alberte, C. de Rham, S. Jaitly and A.J. Tolley, *QED positivity bounds*, *Phys. Rev. D* **103** (2021) 125020 [[2012.05798](#)].

- [64] A. Baldazzi, R.B.A. Zinati and K. Falls, *Essential renormalisation group*, *SciPost Phys.* **13** (2022) 085 [2105.11482].
- [65] A. Baldazzi and K. Falls, *Essential Quantum Einstein Gravity*, *Universe* **7** (2021) 294 [2107.00671].
- [66] “xAct: Efficient tensor computer algebra for Mathematica.” <http://xact.es/index.html>.
- [67] D. Brizuela, J.M. Martin-Garcia and G.A. Mena Marugan, *xPert: Computer algebra for metric perturbation theory*, *Gen. Rel. Grav.* **41** (2009) 2415 [0807.0824].
- [68] T. Nutma, *xTras : A field-theory inspired xAct package for mathematica*, *Comput. Phys. Commun.* **185** (2014) 1719 [1308.3493].
- [69] B. Knorr, *One-Loop Renormalization of Cubic Gravity in Six Dimensions*, *Phys. Rev. Lett.* **128** (2022) 161301 [2109.09857].
- [70] B. Knorr, *Safe essential scalar-tensor theories*, 2204.08564.
- [71] A. Baldazzi, K. Falls, Y. Kluth and B. Knorr, *Robustness of the derivative expansion in Asymptotic Safety*, 2312.03831.
- [72] B. Knorr and A. Platania, “Supplementary Material for "Unearthing the intersections: positivity bounds, weak gravity conjecture, and asymptotic safety landscapes from photon-graviton flows"." Mendeley Data, <http://dx.doi.org/10.17632/tysd636dn4.1>.
- [73] A. Baldazzi, R. Percacci and V. Skrinjar, *Wicked metrics*, *Class. Quant. Grav.* **36** (2019) 105008 [1811.03369].
- [74] E. Manrique and M. Reuter, *Bare versus Effective Fixed Point Action in Asymptotic Safety: The Reconstruction Problem*, *PoS CLAQG08* (2011) 001 [0905.4220].
- [75] T.R. Morris and Z.H. Slade, *Solutions to the reconstruction problem in asymptotic safety*, *JHEP* **11** (2015) 094 [1507.08657].
- [76] M. Fraaije, A. Platania and F. Saueressig, *On the reconstruction problem in quantum gravity*, *Phys. Lett. B* **834** (2022) 137399 [2206.10626].
- [77] A. Eichhorn, A.O. Pedersen and M. Schiffer, *to appear*, .
- [78] A. Codello and R. Percacci, *Fixed points of higher derivative gravity*, *Phys. Rev. Lett.* **97** (2006) 221301 [hep-th/0607128].
- [79] R.C. Myers and J.Z. Simon, *Black Hole Thermodynamics in Lovelock Gravity*, *Phys. Rev. D* **38** (1988) 2434.
- [80] R.C. Myers, *Black holes in higher curvature gravity*, in *Black Holes, Gravitational Radiation and the Universe: Essays in Honor of C.V. Vishveshwara*, B.R. Iyer and B. Bhawal, eds., pp. 121–136 (1998), DOI [gr-qc/9811042].
- [81] T. Clunan, S.F. Ross and D.J. Smith, *On Gauss-Bonnet black hole entropy*, *Class. Quant. Grav.* **21** (2004) 3447 [gr-qc/0402044].
- [82] T. Azeanagi, G. Compere, N. Ogawa, Y. Tachikawa and S. Terashima, *Higher-Derivative Corrections to the Asymptotic Virasoro Symmetry of 4d Extremal Black Holes*, *Prog. Theor. Phys.* **122** (2009) 355 [0903.4176].
- [83] A. Platania and J. Redondo-Yuste, *Diverging black hole entropy from quantum infrared non-localities*, 2303.17621.

- [84] D.F. Litim and J.M. Pawłowski, *Flow equations for Yang-Mills theories in general axial gauges*, *Phys.Lett.* **B435** (1998) 181 [[hep-th/9802064](#)].
- [85] J.L. Cardy, *Is There a c Theorem in Four-Dimensions?*, *Phys. Lett. B* **215** (1988) 749.
- [86] S. Weinberg, *Ultraviolet divergences in quantum theories of gravitation*, *General Relativity: An Einstein centenary survey*, Eds. Hawking, S.W., Israel, W; Cambridge University Press (1979) 790.
- [87] A. Eichhorn, J.H. Kwapisz and M. Schiffer, *Weak-gravity bound in asymptotically safe gravity-gauge systems*, *Phys. Rev. D* **105** (2022) 106022 [[2112.09772](#)].
- [88] G.P. de Brito, B. Knorr and M. Schiffer, *On the weak-gravity bound for a shift-symmetric scalar field*, *Phys. Rev. D* **108** (2023) 026004 [[2302.10989](#)].
- [89] H. Gies and J. Schirmer, *Renormalization Flow of Nonlinear Electrodynamics*, [2405.06472](#).
- [90] N. Christiansen and A. Eichhorn, *An asymptotically safe solution to the U(1) triviality problem*, *Phys. Lett.* **B770** (2017) 154 [[1702.07724](#)].
- [91] H. Gies, B. Knorr and S. Lippoldt, *Generalized Parametrization Dependence in Quantum Gravity*, *Phys. Rev.* **D92** (2015) 084020 [[1507.08859](#)].
- [92] A. Conroy, A. Mazumdar and A. Teimouri, *Wald Entropy for Ghost-Free, Infinite Derivative Theories of Gravity*, *Phys. Rev. Lett.* **114** (2015) 201101 [[1503.05568](#)].
- [93] T. Draper, B. Knorr, C. Ripken and F. Saueressig, *Finite Quantum Gravity Amplitudes: No Strings Attached*, *Phys. Rev. Lett.* **125** (2020) 181301 [[2007.00733](#)].
- [94] A. Guerrieri, J. Penedones and P. Vieira, *Where Is String Theory in the Space of Scattering Amplitudes?*, *Phys. Rev. Lett.* **127** (2021) 081601 [[2102.02847](#)].
- [95] A. Guerrieri, H. Murali, J. Penedones and P. Vieira, *Where is M-theory in the space of scattering amplitudes?*, *JHEP* **06** (2023) 064 [[2212.00151](#)].
- [96] C. Wetterich, *Exact evolution equation for the effective potential*, *Phys.Lett.* **B301** (1993) 90.
- [97] T.R. Morris, *The Exact renormalization group and approximate solutions*, *Int. J. Mod. Phys.* **A9** (1994) 2411 [[hep-ph/9308265](#)].
- [98] U. Ellwanger, *Flow equations for N point functions and bound states*, *Z. Phys. C* **62** (1994) 503 [[hep-ph/9308260](#)].
- [99] J.M. Pawłowski and M. Reichert, *Quantum Gravity: A Fluctuating Point of View*, *Front. in Phys.* **8** (2021) 551848 [[2007.10353](#)].
- [100] F.J. Wegner, *Some invariance properties of the renormalization group*, *Journal of Physics C: Solid State Physics* **7** (1974) 2098.
- [101] J.M. Pawłowski, *Aspects of the functional renormalisation group*, *Annals Phys.* **322** (2007) 2831 [[hep-th/0512261](#)].
- [102] C. Wetterich, *Effective nonlocal Euclidean gravity*, *Gen. Rel. Grav.* **30** (1998) 159 [[gr-qc/9704052](#)].
- [103] H. Gies and C. Wetterich, *Renormalization flow of bound states*, *Phys. Rev. D* **65** (2002) 065001 [[hep-th/0107221](#)].
- [104] F. Ihssen and J.M. Pawłowski, *Flowing fields and optimal RG-flows*, [2305.00816](#).

- [105] C. Wetterich, *Field transformations in functional integral, effective action and functional flow equations*, [2402.04679](#).
- [106] D.F. Litim, *Optimized renormalization group flows*, *Phys.Rev.* **D64** (2001) 105007 [[hep-th/0103195](#)].